PHYSICAL REVIEW D **71,** 014015 (2005)

New results on $B \to \pi, K, \eta$ decay form factors from light-cone sum rules

Patricia Ball[1,*] and Roman Zwicky[2,†]

[1] *IPPP, Department of Physics, University of Durham, Durham DH1 3LE, United Kingdom*

[2] *William I. Fine Theoretical Physics Institute, University of Minnesota, Minneapolis, Minnesota 55455, USA*

(Received 22 June 2004; published 18 January 2005)

We present an improved calculation of $B \to$ light pseudoscalar form factors from light-cone sum rules, including one-loop radiative corrections to twist-2 and twist-3 contributions, and leading-order twist-4 corrections. The total theoretical uncertainty of our results at zero momentum transfer is 10 to 13% and can be improved, at least in part, by reducing the uncertainty of hadronic input parameters, in particular, those describing the twist-2 distribution amplitudes of the π, K, and η. We present our results in a way which details the dependence of the form factors on these parameters and facilitates the incorporation of future updates of their values from, e.g., lattice calculations.

DOI: 10.1103/PhysRevD.71.014015 PACS numbers: 12.38.Lg, 13.20.–v

I. INTRODUCTION

This paper aims to give a new and more precise determination of the decay form factors of B mesons into light pseudoscalar mesons, i.e. π, K, and η. We do not include the η' which is too heavy to be treated in this framework. The calculation uses the method of QCD sum rules on the light-cone, which in the past has been rather successfully applied to various problems in heavy-meson physics cf. Refs. [1–5][1]; an outline of the method will be given below. Our calculation improves on our previous papers [3,4] by

(i) including radiative corrections to twist-3 contributions to one-loop accuracy, for all form factors;
(ii) a precisely defined method for fixing the sum rule specific parameters;
(iii) using updated values for input parameters;
(iv) a careful analysis of the uncertainties of the form factors at zero momentum transfer;
(v) a new parametrization of the dependence of the form factors on momentum transfer, which is consistent with the constraints from analyticity and heavy-quark expansion;
(vi) detailing the dependence of form factors on nonperturbative hadronic parameters describing the π, K, η mesons, the so-called Gegenbauer moments, which facilitates the incorporation of future updates of their numerical values and also allows a consistent treatment of their effect on nonleptonic decays treated in QCD factorization.

The motivation for this study is twofold and related to the overall aim of B physics to provide precision determinations of quark flavor mixing parameters in the standard model. Quark flavor mixing is governed by the unitary Cabibbo-Kobayashi-Maskawa (CKM) matrix which depends on four parameters: three angles and one phase. The constraints from unitarity can be visualized by the so-called unitarity triangles (UT); the one that is relevant for B physics is under intense experimental study. The over-determination of the sides and angles of this triangle from a multitude of processes will answer the question whether there is new physics in flavor-changing processes and where it manifests itself. One of the sides of the UT is given by the ratio of CKM matrix elements $|V_{ub}/V_{cb}|.|V_{cb}|$ is known to about 2% accuracy from both inclusive and exclusive $b \to c\ell\nu$ transitions [7], whereas the present error on $|V_{ub}|$ is much larger and around 15%. Its reduction requires an improvement of experimental statistics, which is underway at the B factories *BABAR* and Belle, but also and, in particular, an improvement of the theoretical prediction for associated semileptonic spectra and decay rates. This is the first motivation for our study of the $B \to \pi$ decay form factor $f_+^{B\to\pi}$, which, in conjunction with alternative calculations, in particular, from lattice [8], will help to reduce the uncertainty from exclusive semileptonic determinations of $|V_{ub}|$. Second, form factors of general $B \to$ light meson transitions are also needed as ingredients in the analysis of nonleptonic two-body B decays, e.g., $B \to K\pi$, in the framework of QCD factorization [9], again with the objective to extract CKM parameters. One issue calling for particular attention in this context is the effect of SU(3) breaking, which enters both the form factors and the K and η meson distribution amplitudes figuring in the factorization analysis. We would like to stress here that the implementation of SU(3) breaking in the light-cone sum rules approach to form factors is *precisely* the same as in QCD factorization and is encoded in the difference between π, K, and η distribution amplitudes, so that the use of form factors calculated from light-cone sum rules together with the corresponding meson distribution amplitudes in factorization formulas allows a unified and controlled approach to the assessment of SU(3) breaking effects in nonleptonic B decays.

As we shall detail below, QCD sum rules on the light-cone allow the calculation of form factors in a kinematic

*Electronic address: Patricia.Ball@durham.ac.uk
†Electronic address: zwicky@physics.umn.edu

[1] See also Ref. [6] for reviews.

regime where the final-state meson has large energy in the rest-system of the decaying B, $E \gg \Lambda_{\rm QCD}$. This is in contrast to lattice calculations which presently are available only for $B \to \pi$ and $q^2 > 15$ GeV^2, due to the restriction to π energies smaller than the inverse lattice spacing.[2] First unquenched results are underway [10,11], which, once published, will allow one to exploit the complementarity of lattice simulations and light-cone sum rules in more detail.

The physics underlying B decays into light mesons at large momentum transfer can be understood qualitatively in the framework of hard exclusive QCD processes, pioneered by Brodsky and Lepage *et al.* [12]. The hard scale in B decays is m_b and one can show that to leading order in $1/m_b$ the decay is described by two different parton configurations: one where all quarks have large momenta and the momentum transfer happens via the exchange of a hard gluon, the so-called hard-gluon exchange, and a second one where one quark is soft and does interact with the other partons only via soft-gluon exchange, the so-called soft or Feynman-mechanism. The consistent treatment of both effects in a framework based on factorization, i.e., the clean separation of perturbatively calculable hard contributions from nonperturbative "wave functions," is highly nontrivial and has spurred the development of SCET, an effective field theory which aims to separate the two relevant large mass scales m_b and $\sqrt{m_b \Lambda_{\rm QCD}}$ in a systematic way [13]. In this approach form factors can indeed be split into a calculable factorizable part which roughly corresponds to the hard-gluon exchange contributions, and a nonfactorizable one, which includes the soft contributions and cannot be calculated within the SCET framework [14]. Predictions obtained in this approach then typically aim to eliminate the soft part and take the form of relations between two or more form factors whose difference is expressed in terms of factorizable contributions.

The above discussion highlights the need for a calculational method that allows numerical predictions while treating both hard and soft contributions on the same footing. It is precisely QCD sum rules on the light-cone (LCSRs) that accomplish this task. LCSRs can be viewed as an extension of the original method of QCD sum rules devised by Shifman, Vainshtein and Zakharov (SVZ) [15], which was designed to determine properties of ground-state hadrons at zero or low momentum transfer, to the regime of large momentum transfer. QCD sum rules combine the concepts of operator product expansion, dispersive representations of correlation functions, and quark-hadron duality in an ingenuous way that allows the calculation of the properties of nonexcited hadron-states with a very reasonable theoretical uncertainty. In the context of weak-decay form factors, the basic quantity is the correlation function of the weak current and a current with the quantum numbers of the B meson, evaluated between the vacuum and a light meson. For large (negative) virtualities of these currents, the correlation function is, in coordinate-space, dominated by distances close to the light-cone and can be discussed in the framework of light-cone expansion. In contrast to the short-distance expansion employed by conventional QCD sum rules à la SVZ where nonperturbative effects are encoded in vacuum expectation values of local operators with vacuum quantum numbers, the condensates, LCSRs rely on the factorization of the underlying correlation function into genuinely nonperturbative and universal hadron distribution amplitudes (DAs) ϕ which are convoluted with process-dependent amplitudes T. The latter are the analogues of the Wilson-coefficients in the short-distance expansion and can be calculated in perturbation theory. The light-cone expansion then reads, schematically:

$$\text{correlation function} \sim \sum_n T^{(n)} \otimes \phi^{(n)}. \tag{1}$$

The sum runs over contributions with increasing twist, labeled by n, which are suppressed by increasing powers of, roughly speaking, the virtualities of the involved currents. The same correlation function can, on the other hand, be written as a dispersion relation, in the virtuality of the current coupling to the B meson. Equating dispersion-representation and the light-cone expansion, and separating the B meson contribution from that of higher one- and multiparticle states using quark-hadron duality, one obtains a relation for the form factor describing the decay $B \to$ light meson.

One crucial question is the accuracy of the resulting predictions for form factors. Evidently light-cone sum rules depend on a number of input parameters, notably quark masses and distribution amplitudes, which induce a (reducible) theoretical uncertainty. In addition, the approximations inherent in the method, in particular, the modeling of the contribution of higher-mass states to the correlation function, also induce a systematic (irreducible) uncertainty. For the form factors calculated in this paper, we find that the total theoretical uncertainty at $q^2 = 0$ is 10 to 13%, and could be reduced to less than 10% with improved input parameters.

Our paper is organized as follows: in Sec. II we define all relevant quantities, in particular, correlation functions and meson distribution amplitudes. In Sec. III we outline our calculations and derive the light-cone sum rules. In Sec. IV we present our numerical results and give a detailed discussion of their uncertainty. Section V contains a summary and conclusions. Detailed expressions for

[2]This situation may change in the future with the successful implementation of "moving NRQCD" [10], where the B decays while moving "backwards," which gives access to smaller values of q^2 without increasing the discretization error.

distribution amplitudes and explicit formulas for the light-cone sum rules are given in the appendices.

II. DEFINITIONS

The form factors f_+^P, f_0^P, and f_T^P which are relevant for the $B \to P$ transition, where P stands for π, K, or η, are defined as follows:[3]

$$\langle P(p)|V_\mu^P|B(p_B)\rangle = \left\{(p + p_B)_\mu - \frac{m_B^2 - m_P^2}{q^2} q_\mu\right\} f_+^P(q^2) + \left\{\frac{m_B^2 - m_P^2}{q^2} q_\mu\right\} f_0^P(q^2), \qquad (2)$$

$$\langle P(p)|J_\mu^{P,\sigma}|B(p_B)\rangle = \frac{i}{m_B + m_P}\{q^2(p + p_B)_\mu - (m_B^2 - m_P^2)q_\mu\} f_T^P(q^2, \mu), \quad (3)$$

where $V_\mu^{\pi,\eta} = \bar{u}\gamma_\mu b$ is the standard weak current, V_μ^K is given by $V_\mu^K = \bar{s}\gamma_\mu b$, and $J_\mu^{\pi(\eta),\sigma} = \bar{d}\sigma_{\mu\nu}q^\nu b$, $J_\mu^{K,\sigma} = \bar{s}\sigma_{\mu\nu}q^\nu b$ are penguin currents. The momentum transfer is given by $q = p_B - p$ and the physical range in q^2 is $0 \le q^2 \le (m_B - m_P)^2$. The form factors f_+^P and f_0^P are independent of the renormalization scale μ since V_μ is a physical current, in contrast to the penguin current J_μ^σ. Note that $f_+^P(0) = f_0^P(0)$ which is a consequence of the parametrization chosen in Eq. (2). We assume SU(2) isospin symmetry throughout this work, i.e., we do not distinguish $\bar{B}^0 \to \pi^+$ and $B^- \to \pi^0$ form factors, etc.

In the semileptonic decay $B \to \pi l \nu_l$ the form factor f_0^π enters proportional to the lepton mass m_l^2 and hence is irrelevant for light leptons ($l = e, \mu$), where only f_+^π matters. The semileptonic decay can be used to determine the size of the CKM matrix element $|V_{ub}|$ from the spectrum

$$\frac{d\Gamma}{dq^2}(B \to \pi l \nu_l) = \frac{G_F^2|V_{ub}|^2}{192\pi^3 m_B^3}\lambda(q^2)^{3/2}|f_+^\pi(q^2)|^2, \qquad (4)$$

where $\lambda(x) = (x + m_B^2 - m_\pi^2)^2 - 4xm_B^2$. The form factor f_0^π will be relevant in and can be measured from the decay $B \to \pi\tau\nu_\tau$. f_T^π is relevant for the rare decay $B \to \pi l^+ l^-$, where the penguin current features in the effective Hamiltonian of the process.

Our starting point for calculating the form factors $f_{+,0}^\pi$ is the correlation function

$$\Pi_\mu(q, p_B) = i\int d^4x e^{iq\cdot x}\langle\pi(p)|TV_\mu(x)j_B^\dagger(0)|0\rangle = \Pi_+(q^2, p_B^2)(p + p_B)_\mu + \Pi_-(q^2, p_B^2)q_\mu, \qquad (5)$$

where $j_B = m_b\bar{d}i\gamma_5 b$ is the interpolating field for the B meson. For the calculation of f_T^π, V_μ has to be replaced by J_μ^σ. For virtualities

$$m_b^2 - p_B^2 \ge O(\Lambda_{\rm QCD}m_b), \qquad m_b^2 - q^2 \ge O(\Lambda_{\rm QCD}m_b), \qquad (6)$$

the correlation function (5) is dominated by lightlike distances and therefore accessible to an expansion around the light-cone. The above conditions can be understood by demanding that the exponential factor in (5) vary only slowly. The light-cone expansion is performed by integrating out the transverse and "minus" degrees of freedom and leaving only the longitudinal momenta of the partons as relevant degrees of freedom. The integration over transverse momenta is done up to a cutoff, $\mu_{\rm IR}$, all momenta below which are included in a so-called hadron distribution amplitude ϕ, whereas larger transverse momenta are calculated in perturbation theory. The correlation function is hence decomposed, or factorized, in perturbative contributions T and nonperturbative contributions ϕ, which both depend on the longitudinal parton momenta and the factorization scale $\mu_{\rm IR}$. If the π is an effective quark-antiquark bound state, as is the case to leading order in the light-cone expansion, we can write the corresponding longitudinal momenta as up and $(1-u)p$, p being the momentum of the π. The schematic relation (1) can then be written in more explicit form as

$$\Pi_+(q^2, p_B^2) = \sum_n \int_0^1 du T^{(n)}(u, q^2, p_B^2, \mu_{\rm IR})\phi^{(n)}(u, \mu_{\rm IR}). \qquad (7)$$

As Π_+ itself is independent of the arbitrary scale $\mu_{\rm IR}$, the scale dependence of $T^{(n)}$ and $\phi^{(n)}$ must cancel each other.[4] If $\phi^{(n)}$ describes the meson in a two-parton state, it is called a two-particle distribution amplitude (DA), if it describes a three-parton, i.e., quark-antiquark-gluon state, it is called three-particle DA. In the latter case the integration over u gets replaced by an integration over two independent momentum fractions, say α_1 and α_2. Equation (7) is called a "collinear" factorization formula, as the momenta of the partons in the π are collinear with the π's momentum, and its validity actually has to be verified. We will come back to that issue in the next section.

Let us now define the distribution amplitudes to be used in this paper. Again we only quote formulas for the π meson, those for the K and η are analogous. All definitions and formulas are well-known and can be found in Ref. [16]. In general, the distribution amplitudes we are interested in are related to nonlocal matrix elements of

[3]The following notations are frequently used in the literature: $f_+ = F_1$ and $f_0 = F_0$.

[4]If there is more than one contribution of a given twist, they will mix under a change of the factorization scale $\mu_{\rm IR}$ and it is only in the sum of all such contributions that the residual $\mu_{\rm IR}$ dependence cancels.

type

$$\langle 0|\bar{u}(x)\Gamma[x,-x]d(-x)|\pi(p)\rangle \quad \text{or} \quad \langle 0|\bar{u}(x)[x,vx]\Gamma G^a_{\mu\nu}(vx)\lambda^a/2[vx,-x]d(-x)|\pi(p)\rangle.$$

x is lightlike or close to lightlike and the light-cone expansion is an expansion in x^2; v is a number between 0 and 1 and Γ a combination of Dirac matrices. The expressions $[x,-x]$, etc. denote Wilson lines that are needed to render the matrix elements, and hence the DAs, gauge-invariant. One usually works in the convenient Fock-Schwinger gauge $x^\mu A^a_\mu(x)\lambda^a/2 = 0$, where all Wilson lines are just $\mathbf{1}$; we will suppress them from now on. The DAs are ordered by twist, i.e., the difference between spin and dimension of the corresponding operators. We will include DAs of twist-2 (the leading twist), -3, and -4. The leading-twist DA ϕ_π is defined as

$$\begin{aligned}\langle 0|\bar{u}(x)\gamma_\mu\gamma_5 d(-x)|\pi^-(p)\rangle &= if_\pi p_\mu \int_0^1 du e^{i\zeta p\cdot x} \\ &\quad \times\left[\phi_\pi(u) + \frac{1}{4}m_\pi^2 x^2 \mathbb{A}(u)\right] \\ &\quad + if_\pi \frac{m_\pi^2}{px} x_\mu \int_0^1 du e^{i\zeta p\cdot x} \\ &\quad \times g_\pi(u) + O(x_\mu x^2) \end{aligned} \tag{8}$$

with $\zeta \equiv 2u-1$ and $p^2 = 0$. The above matrix element also contains two twist-4 DAs, g_π and $\mathbb{A}$. The variable u can be interpreted as the momentum fraction carried by the quark (as opposed to the antiquark) in the meson.

There are two two-particle twist-3 DAs, ϕ_p and ϕ_σ, which are defined as

$$\langle 0|\bar{u}(x)i\gamma_5 d(-x)|\pi(p)\rangle = \mu_\pi^2 \int_0^1 du e^{i\zeta p\cdot x}\phi_p(u), \tag{9}$$

$$\begin{aligned}\langle 0|\bar{u}(x)i\sigma_{\mu\nu}\gamma_5 d(-x)|\pi(p)\rangle &= -\frac{i}{3}\mu_\pi^2(1-\rho_\pi^2) \\ &\quad \times(p_\mu x_\nu - x_\mu p_\nu) \\ &\quad \times \int_0^1 du e^{i\zeta p\cdot x}\phi_\sigma(u), \end{aligned} \tag{10}$$

where $\mu_\pi^2 \equiv f_\pi m_\pi^2/(m_u + m_d)$ and $\rho_\pi^2 \equiv (m_u + m_d)^2/m_\pi^2$.

The precise definitions of three-particle DAs are a bit cumbersome and given in App. B. The salient feature is that there is one three-particle DA of twist-3 and four of twist-4.

Although we have introduced not less than ten different DAs, which are all nonperturbative quantities, it may seem, at first glance, that light-cone sum rules do not retain much predictive power. Fortunately, however, it turns out that the DAs are highly constrained functions which can be analyzed in the framework of conformal expansion, a topic being discussed in App. B. The main result is that, to next-to-leading-order in conformal expansion, which is sufficient for the accuracy we are aiming at, all ten DAs can be expressed in terms of seven independent hadronic parameters.

This completes the definitions necessary for the calculation of form factors.

III. THE SUM RULES

The diagrams to be calculated to $O(\alpha_s)$ for two-particle DAs are shown in Fig. 1. The quark (antiquark) is collinear with the light meson and carries momentum up ($(1-u)p$). Quarks are projected onto the corresponding distribution amplitudes using the completeness relation

$$\begin{aligned}\bar{u}_a d_b &= \frac{1}{4}(\mathbf{1})_{ba}(\bar{u}d) - \frac{1}{4}(i\gamma_5)_{ba}(\bar{u}i\gamma_5 d) + \frac{1}{4}(\gamma_\mu)_{ba}(\bar{u}\gamma^\mu d) \\ &\quad - \frac{1}{4}(\gamma_\mu\gamma_5)_{ba}(\bar{u}\gamma^\mu\gamma_5 d) + \underbrace{\frac{1}{8}(\sigma_{\mu\nu})_{ba}(\bar{u}\sigma^{\mu\nu}d)}_{\equiv -\frac{1}{8}(\sigma_{\mu\nu}i\gamma_5)_{ba}(\bar{u}\sigma^{\mu\nu}i\gamma_5 d)}.\end{aligned}$$

The diagrams are calculated in momentum space. The terms in x_μ in the contribution of ϕ_σ, Eq. (10), are rewritten in terms of derivatives

$$x_\mu \longrightarrow -i\frac{\partial}{\partial(up)_\mu}.$$

In the previous section we mentioned that the fact that Π can be written in factorized form cannot be taken for granted, but requires proof. We do not attempt to give a proof to all orders in α_s, although that should be possible using the techniques of SCET, but restrict ourselves to $O(\alpha_s)$ in twist-2, to all orders in the conformal expansion, and to $O(\alpha_s)$ and leading order in the conformal expansion for twist-3. The proof essentially relies on the cancellation of singularities, of which there are several possible types: infrared and ultraviolet singularities arising from loop calculations and so-called soft singularities which occur when the integral over u in Eq. (7) does diverge at the endpoints. The latter divergences have actually posed a severe problem in early attempts to treat f_+^π in QCD factorization: in Ref. [17] only the hard-gluon exchange was included, which yields a logarithmic divergence for the parton configuration where the u quark emerging from the weak decay carries essentially all

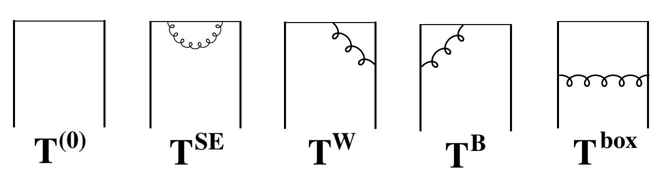

FIG. 1. Perturbative contributions to the correlation function Π. The external quarks are on-shell with momenta up and $(1-u)p$, respectively.

pion momentum. As we understand now, this divergence disappears when contributions from the Feynman-mechanism are added. In our case, it turns out that all T are regular at the endpoints $u = 0, 1$, so there are *no soft divergences, independent of the end point behavior of the distribution amplitudes.* As for infrared and ultraviolet singularities, they can be treated in dimensional regularization. Using the lowest-order expression of the Brodsky-Lepage evolution kernel for ϕ_π derived in [12], we have followed the strategy outlined in [18] to check that the infrared divergences precisely cancel those contained in the bare DA $\phi_\pi^{\rm bare}$. As for twist-3, the evolution kernel is not known, so we have only checked the cancellation of infrared divergences of the lowest-order term in the conformal expansion, whose divergent behavior is well-known—in fact, only the one-loop renormalization of the quark condensate is needed. The ultraviolet divergences cancel for f_+ and f_0, which are physical form factors and hence do not depend on the ultraviolet renormalization scale; for f_T, we reproduce the well-known one-loop anomalous dimension.

We then have used the explicit expressions for the twist-2 and three two-particle DAs given in App. B to perform the integration over u analytically. Actually it is not the correlation function Π itself that is needed, but its imaginary part, see below. Π has a cut in p_B^2 starting at m_b^2 and taking the imaginary part after integration over u is straightforward. The strategy outlined here is different from the procedure we followed in our previous papers [3,4], where we took the imaginary part before integrating over u. This latter procedure resulted in expressions with a very complicated analytical structure which made it impossible to give explicit formulas for the imaginary parts. With our new procedure we obtain lengthy, but not very complicated expressions; the complete set of spectral densities $\rho = ({\rm Im}\Pi)/\pi$ for the sum rule for the form factor f_+ is given in App. C.

Armed with the spectral densities, we can derive the LCSR for, e.g., the form factor f_+. The basic quantity is Π_+, which is calculated in two ways. In light-cone expansion, it can be written in dispersive representation as

$$\Pi_+^{\rm LC}(p_B^2, q^2) = \int_{m_b^2}^{\infty} ds \frac{\rho_+^{\rm LC}(s, q^2)}{s - p_B^2} \qquad (11)$$

with the explicit expression for the spectral density $\rho_+^{\rm LC}(s)$ given in App. C. This expression has to be compared to the physical correlation function, which also features a cut in p_B^2, starting at m_B^2:

$$\Pi_+^{\rm phys}(p_B^2, q^2) = \int_{m_B^2}^{\infty} ds \frac{\rho_+^{\rm phys}(s, q^2)}{s - p_B^2}; \qquad (12)$$

the spectral density is given by hadronic contributions and reads

$$\rho_+^{\rm phys}(s, q^2) = f_B m_B^2 f_+(q^2) \delta(s - m_B^2) + \rho_+^{\rm higher-mass\ states}(s, q^2). \qquad (13)$$

Here f_B is the B meson decay constant defined as

$$\langle 0|\bar{q}\gamma_\mu\gamma_5 b|B\rangle = i f_B p_\mu \quad \text{or} \quad (m_b + m_q)\langle 0|\bar{q} i\gamma_5 b|B\rangle = m_B^2 f_B. \qquad (14)$$

To obtain a light-cone sum rule for f_+, one equates the two expressions for Π_+ and uses quark-hadron duality to approximate

$$\rho_+^{\rm higher-mass\ states}(s, q^2) \approx \rho_+^{\rm LC}(s, q^2)\Theta(s - s_0), \qquad (15)$$

where s_0, the so-called continuum threshold is a parameter to be determined within the sum rule approach itself. In principle one could now write a sum rule

$$\Pi_+^{\rm phys}(p_B^2, q^2) = \Pi_+^{\rm LC}(p_B^2, q^2)$$

and determine f_+ from it. However, in order to suppress the impact of the approximation (15), one subjects both sides of the equation to a Borel transformation

$$\frac{1}{s - p_B^2} \to \hat{B}\frac{1}{s - p_B^2} = \frac{1}{M^2}\exp(-s/M^2)$$

which ensures that contributions from higher-mass states be sufficiently suppressed and improves the convergence of the OPE. We then obtain

$$e^{-m_B^2/M^2} m_B^2 f_B f_+(q^2) = \int_{m_b^2}^{s_0} ds e^{-s/M^2} \rho_+^{\rm LC}(s, q^2). \qquad (16)$$

This is the final sum rule for f_+; expressions for the other form factors are obtained analogously. The task now is to find sets of parameters M^2 (the Borel parameter) and s_0 (the continuum threshold) such that the resulting form factor does not depend too much on the precise values of these parameters; in addition the continuum contribution, that is the part of the dispersive integral from s_0 to ∞ that has been subtracted from both sides of (16), should not be too large, say less than 30% of the total dispersive integral.

IV. NUMERICS

In this section we obtain numerical results from the sum rules (16). The section is organized as follows: in Sec. IV A we explain how we determine the sum rule specific parameters, i.e., the Borel parameter M^2 and the continuum threshold s_0. We also determine f_B, which is a necessary ingredient in (16). In Sec. IV B we explain in more detail how we fix the hadronic input parameters, in particular, the Gegenbauer moments $a_{1,2,4}$ that describe the final-state mesons. In Sec. IV C we calculate the form factors at $q^2 = 0$ and discuss their uncertainties. In Sec. IV D we present the form factors for central input values of the parameters and provide a simple parametri-

TABLE I. Final central values of the form factors at $q^2 = 0$ for the parameter sets of Table III. $f_0(0) \equiv f_+(0)$. The errors Δ_{as}, Δ_{a_2,a_4}, and Δ_{a_1} are described in the text. Δ is defined as $\Delta = (\Delta_{as}^2 + \Delta_{a_2,a_4}^2)^{1/2}$ and δ_{a_1} as $\delta_{a_1} = a_1(1\text{ GeV}) - 0.17$. Note that δ_{a_1} carries information on the sign of a_1 and can become negative.

	set 1	set 2	set 3	set 4	Δ_{as}	Δ_{a_2,a_4}	Δ	Δ_{a_1}
$f_+^\pi(0)$	0.250	0.258	0.263	0.274	0.023	0.019	0.030	—
$f_T^\pi(0)$	0.244	0.253	0.260	0.273	0.013	0.022	0.026	—
$f_+^K(0)$	0.324	0.331	0.335	0.339	0.033	0.023	0.040	$0.25\delta_{a_1}$
$f_T^K(0)$	0.347	0.358	0.367	0.381	0.022	0.027	0.035	$0.31\delta_{a_1}$
$f_+^\eta(0)$	0.269	0.275	0.278	0.286	0.029	0.019	0.035	—
$f_T^\eta(0)$	0.277	0.285	0.292	0.305	0.018	0.022	0.028	—

zation valid in the full kinematical regime of q^2. The results for $q^2 = 0$ are collected in Table I and Eq. (27), central results for arbitrary q^2 in Table II. More detailed results that allow one to determine the form factors for arbitrary values of m_b and the Gegenbauer moments $a_{1,2,4}$ are collected in App. A.

A. Fixing the Borel Parameter and the Continuum Threshold

We illustrate our procedure to determine M^2 and s_0 with the comparatively simple example of f_B, the B decay constant defined in (14). This example is actually of immediate practical use, as f_B enters our determination of the form factors from Eq. (16). Since it is not known from experiment, its value has to be taken from theoretical calculations—which basically means either lattice determinations [19] or (local) QCD sum rules [20,21]. To ensure consistency of our calculations, we use the values of f_B as determined from QCD sum rules to $O(\alpha_s)$ accuracy [20]. The reason for this choice is two-fold: first, it is well-known that the use of f_B from sum rules reduces the dependence of the form factors on input parameters, in particular m_b [1]; second, $O(\alpha_s^2)$ corrections to f_B turn out to be rather large [21], which was anticipated in the second reference in [20], where it was argued that these corrections are dominated by Coulombic corrections. Precisely the same corrections also enter the light-cone expansion of the correlation function Π, but will largely cancel in the ratio $f_+ \sim \Pi/f_B$. In conclusion, we expect a cancellation of both large radiative corrections and parameter dependence in the form factors when f_B is replaced by its sum rule to $O(\alpha_s)$ accuracy; we do not expect the resulting numerical values of f_B to be "good" predictions for that quantity.

TABLE II. Fit parameters for Eq. (30) for set 2 in Table III and central values of the input parameters of the DAs, Eqs. (24) and (25) and Table IV. m_1 is the vector-meson mass in the corresponding channel: $m_1^{\pi,\eta} = m_{B^*} = 5.32$ GeV and $m_1^K = m_{B_s^*} = 5.41$ GeV. The scale of f_T is $\mu = 4.8$ GeV.

	r_1	r_2	$(m_1)^2$	$m_{\rm fit}^2$
f_+^π	0.744	− 0.486	$(m_1^\pi)^2$	40.73
f_0^π	0	0.258	—	33.81
f_T^π	1.387	− 1.134	$(m_1^\pi)^2$	32.22
f_+^K	0.162	0.173	$(m_1^K)^2$	—
f_0^K	0	0.330	—	37.46
f_T^K	0.161	0.198	$(m_1^K)^2$	—
f_+^η	0.122	0.155	$(m_1^\eta)^2$	—
f_0^η	0	0.273	—	31.03
f_T^η	0.111	0.175	$(m_1^\eta)^2$	—

The sum rule for f_B reads [20][5]

$$
\begin{aligned}
f_B^2 m_B^2 e^{-(m_B^2/M^2)} &= \int_{m_b^2}^{s_0} ds \rho^{\rm pert}(s) e^{-(s/M^2)} + C_{\bar{q}q}\langle\bar{q}q\rangle \\
&\quad + C_{\bar{q}Gq}\langle\bar{q}\sigma gGq\rangle \\
&\equiv \int_{m_b^2}^{s_0} ds \rho^{\rm tot}(s) e^{-(s/M^2)}. \qquad (17)
\end{aligned}
$$

The C are the Wilson-coefficients multiplying the condensates, for which we use the following numerical values at $\mu = 1$ GeV:

$$
\begin{aligned}
\langle\bar{q}q\rangle &= -(0.24 \pm 0.01)^3 \text{ GeV}^3 \quad \text{and} \\
\langle\bar{q}\sigma gGq\rangle &= 0.8 \text{ GeV}^2\langle\bar{q}q\rangle. \qquad (18)
\end{aligned}
$$

The condensates (and α_s) are actually evaluated at the scale $\mu_{\rm IR}^2$. The criteria for determining M^2 and s_0 are often not stated very precisely. In the present context, with many different form factors to calculate, which entails the need for a well-defined procedure to determine the input parameters for each of them, we decide to opt for a precisely defined method to fix the pair (M^2, s_0) and impose the following criteria on the sum rule for f_B (and, later on, the form factors):

(i) the derivative of the logarithm of Eq. (17) with respect to $1/M^2$ gives a sum rule for the B meson mass m_B:

$$m_B^2 = \int_{m_b^2}^{s_0} ds s \rho^{\rm tot}(s) \Big/ \int_{m_b^2}^{s_0} ds \rho^{\rm tot}(s);$$

we require this sum rule to be fullfilled to high accuracy $\sim 0.1\%$.

(ii) the sum rule for f_B is required to exhibit an extremum for a given pair (M^2, s_0).

These criteria define a set of parameters for each value of m_b, which are collected in Table III, together with the resulting f_B. For all these parameter sets the continuum

[5]The contribution of the gluon condensate is not sizable and we therefore neglect it.

TABLE III. Parameter sets for f_B and $f(0)$; we use the same values of c_c and s_0 for π, K, and η. m_b and f_B are given in GeV, s_0 and M^2 in GeV^2.

	m_b	s_0	M^2	f_B	$s_0^+ \approx s_0^0$	c_c^+	s_0^T	c_c^T
set 1	4.85	33.8	3.8	0.150	33.3	2.00	33.6	2.4
set 2	4.80	34.2	4.1	0.162	33.9	2.25	34.3	2.5
set 3	4.75	34.6	4.4	0.174	34.5	2.50	35.1	2.6
set 4	4.60	35.7	5.1	0.210	36.8	3.00	37.8	2.9

contribution (i.e., the integral $\int_{s_0}^{\infty}$) is between 25% and 30% of the B contribution and hence well under control.

For the form factors f_+^π, f_0^π, and f_T^π we follow the same procedure which results in different values of M^2 and s_0 for form factors and f_B. For K and η we use the same values for the Borel parameter and the continuum threshold. From the explicit formulas of the tree-level sum rules for the form factors quoted in, e.g., the Ref. 3 in [1], one finds that the effective Borel parameter is uM_{LC}^2 rather than M_{LC}^2.[6] In order to keep this product constant, we rescale the Borel parameter by $\langle u\rangle^{-1}$ by

$$\langle u\rangle(q^2) \equiv \int_{u_0}^1 du u \frac{\phi_\pi(u)}{u} e^{-[m_b^2-(1-u)q^2]/uM^2} \Big/ \int_{u_0}^1 du \frac{\phi_\pi(u)}{u} e^{-[m_b^2-(1-u)q^2]/uM^2},$$
$$u_0 = \frac{m_b^2 - q^2}{s_0 - q^2},$$

resulting in the approximate values $\langle u\rangle(0\ \mathrm{GeV}^2) = 0.86$ and $\langle u\rangle(14\ \mathrm{GeV}^2) = 0.77$. Parametrizing the relation between the Borel parameters by

$$M_{\mathrm{LC}}^2 \equiv c_c M^2/\langle u\rangle, \tag{19}$$

we obtain the values and continuum thresholds given in Table III.

B. Hadronic Input Parameters

The hadronic parameters needed are, for each meson, seven parameters characterizing the twist-2, -3, and -4 distribution amplitudes to next-to-leading-order (NLO) in the conformal expansion, cf. App. B, the decay constants of the π, K and η and B, the factorization scale μ_{IR}, the b quark mass m_b, and the strong coupling α_s. As for the latter, we fix $\alpha_s(m_Z) = 0.118$ and use NLO evolution down to the required scale. The quark mass parameter entering our formulas is the one-loop pole mass m_b for which we use $m_b = (4.80 \pm 0.05)$ GeV (cf. Table 6 in the recent review [6] and references therein). We also include results for $m_b = 4.6$ GeV. The infrared factorization scale separating contributions to be included in DAs and perturbatively calculable terms is chosen to be $\mu_{\mathrm{IR}}^2 = m_B^2 - m_b^2$, which also sets the scale of α_s; we will discuss the residual scale dependence of our results below. The decay constants for the π and K are very well-known experimentally; for the η the situation is complicated due to η–η' mixing. We use the following values:

$$f_\pi = 131\ \mathrm{MeV}, \qquad f_K = 160\ \mathrm{MeV}, \qquad f_\eta = 130\ \mathrm{MeV}. \tag{20}$$

f_B has been discussed in the previous subsection.

As for the meson DAs, we quote the preferred values for the twist-3 and -4 parameters in Table IV; the form factors are not too sensitive to their precise values. The situation is different, however, for the Gegenbauer moments $a_{1,2,4}(\mu)$ parametrizing the twist-2 DAs $\phi_{\pi,K,\eta}$, and so we shall discuss in a bit more detail what is presently known about these parameters.

Both theoretical calculations and experimental determinations focus mainly on the π DA (for which all odd Gegenbauer moments vanish due to G-parity; in particular $a_1^\pi = 0$). The probably earliest calculation of the lowest Gegenbauer moment a_2 was done by Chernyak and Zhitnitsky (CZ), yielding [22]

$$a_2^{\mathrm{CZ}}(0.5\ \mathrm{GeV}) = 2/3.$$

This result was obtained from local QCD sum rules, where a_n is extracted from the correlation function of the (local) interpolating field $\bar u \gamma_\nu \gamma_5 (\overleftrightarrow{D} \cdot x)^n d$, where x defines the light-cone, $x^2 = 0$, and the usual interpolating current for the π, $\bar u \gamma_\mu \gamma_5 d$. The price to pay for the expansion of an intrinsically nonlocal quantity like ϕ_π in contributions of local operators is an increasing sensitivity to nonperturbative effects, i.e., the precise values of the condensates. As the coefficients of the condensates in the sum rule for a_n increase with powers of n and, for sufficiently large n, dominate over the perturbative contributions, it is clear that this method is inappropriate for calculating high moments, but one might expect it to be reliable at least for the lowest moment with $n = 2$.

The DA obtained by CZ has the remarkable feature that $\phi_\pi(1/2, 0.5\ \mathrm{GeV}) = 0$, which is of course an artifact of neglecting all contributions from $a_{n\geq 4}$. It was subsequently shown by Braun and Filyanov (BF) [23] that both the pion-nucleon-nucleon coupling $g_{\pi NN}$ and its

TABLE IV. Input parameters for twist-3 and -4 DAs, calculated from QCD sum rules. The accuracy is about 50%. Renormalization scale is 1 GeV.

	π	K	η
η_3	0.015	0.015	0.013
ω_3	-3	-3	-3
η_4	10	0.6	0.5
ω_4	0.2	0.2	0.2

[6] We denote the Borel parameter of the LCSR (16) by M_{LC}^2 and the Borel parameter of the SR (17) by M^2.

mesonic equivalent $g_{\rho\omega\pi}$, when calculated from LCSRs, require a value of $\phi_\pi(1/2)$ significantly different from zero (albeit at a slightly different scale):

$$\phi_\pi(1/2, 1\ \text{GeV}) = 1.2 \pm 0.3 = \frac{3}{2} - \frac{9}{4} a_2(1\ \text{GeV}) + \frac{45}{16} a_4(1\ \text{GeV}) + \ldots, \qquad (21)$$

where the dots denote neglected terms in $a_{n\geq 6}$. The large error is due to a large sensitivity of this result to twist-4 corrections to the sum rules. BF also redetermined a_2, using the same procedure as CZ, and combining their result, which is consistent with a_2^{CZ}, with the above constraint from $\phi_\pi(1/2)$, they obtained

$$a_2^{\text{BF}}(1\ \text{GeV}) = 0.44, \qquad a_4^{\text{BF}}(1\ \text{GeV}) = 0.25.$$

An alternative calculation aims to cure the problem of increasing condensate contributions by resumming them into nonlocal condensates [24]. The Gegenbauer moments in this approach are mostly sensitive to the ratio

$$\lambda_q^2 = \langle \bar{q}\sigma g G q\rangle/(2\langle\bar{q}q\rangle) = (0.4 \pm 0.1)\ \text{GeV}^2 \quad (\mu = 1\ \text{GeV})$$

and have moderate to small values. The most recent paper on that topic, Ref. [25], quotes

$$a_2(1.16\ \text{GeV}) = 0.19, \qquad a_4(1.16\ \text{GeV}) = -0.13, \qquad a_{6,8,10} \sim 10^{-3}. \qquad (22)$$

There are not too many lattice calculations of moments of the π DA. The fairly old values quoted in [26] for the 2nd moment suffer from large uncertainties. This quantity has been investigated again recently [27], but the results, obtained in quenched approximation, are still preliminary.

Alternative determinations of Gegenbauer moments rely on the analysis of experimental data, in particular, the pion-photon transition form factor $\gamma + \gamma^* \to \pi$, measured at CLEO and Cello, and the electromagnetic form factor of the pion. The results of these analyses are typically either determinations of a_2 (setting $a_{n\geq 4}$ to 0) or constraints on a linear combination of a_2 and a_4 (setting $a_{n\geq 6}$ to 0).[7] These determinations are limited by mainly two problems: large experimental errors and the contamination by poorly known twist-4 and higher effects, which are usually estimated from QCD sum rules. As for the pion-photon transition form factor, which has been measured by CLEO and Cello, the technique used to extract a_2 and a_4 has been pioneered by Khodjamirian [29], refined by Schmedding and Yakovlev [30], with subsequent further refinements by Bakulev, Mikhailov, and Stefanis [31]. The upshot is that for not too small Q^2 the pion-photon transition is mostly sensitive to a like-sign combination of a_2 and a_4. Summarizing the analyses of this process, we conclude from Table I in [25] that

$$a_2(1\ \text{GeV}) + a_4(1\ \text{GeV}) = 0.1 \pm 0.1 \qquad (23)$$

is a fair reflection of the current state of knowledge of $a_{2,4}$ from that process.

As for the pion electromagnetic form factor, the authors of Ref. [32] unfortunately only obtain a value for a_2 and set a_4 to 0. A very recent analysis of that form factor, Ref. [25], concludes that calculations using the nonlocal-condensate model are in good agreement with data.

So what then do we actually know about a_2 and a_4? It seems to us that, taking everything together, and with due consideration of the respective strengths and weaknesses of different approaches, the most reliable constraints for these quantities are (21) and (23). These two constraints contain opposite-sign combinations of a_2 and a_4 and hence are about equally sensitive to both parameters. The resulting allowed area for a_2 and a_4 is shown in Fig. 2; its center is at

$$a_2(1\ \text{GeV}) = 0.115, \qquad a_4(1\ \text{GeV}) = -0.015,$$
$$a_2(2.2\ \text{GeV}) = 0.080, \qquad a_4(2.2\ \text{GeV}) = -0.0089. \qquad (24)$$

These are the central values we will use in our calculation of form factors. The figure also shows that the remaining uncertainties are still considerable. Anticipating a future better determination of these parameters, from lattice or else, we will present our final results in such a way as to facilitate the inclusion of any shift in these values. Since much less is known about the Gegenbauer moments of the

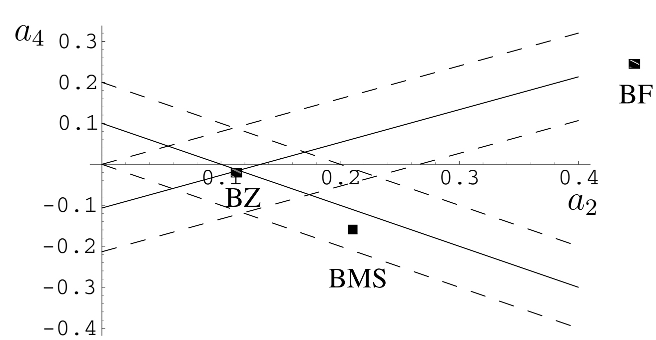

FIG. 2. $a_2(1\ \text{GeV})$ and $a_4(1\ \text{GeV})$ as determined from the constraints (21) and (23). Solid lines: central values; dashed lines: uncertainties. The black square labeled BZ denotes the central values used in this paper, Eq. (24), BMS is the prediction of the nonlocal-condensate model, Eq. (22), rescaled to $\mu = 1$ GeV, and BF is the central value obtained in Ref. [16].

[7]In principle it is possible to determine a_2, a_4 and even higher moments separately from the Q^2 dependence of their respective contributions. However, such an analysis requires accurate measurements of the form factors over a large enough range of Q^2, which are presently not available. See also Ref. [28], in particular, Fig. 4.

other pseudoscalar mesons K and η, we resort to SU(3) symmetry and use *the same* Gegenbauer moments.

Equation (24) and Fig. 2 confirm the findings of previous analyses that the CZ DA is strongly disfavored; the same applies to the values obtained by BF and to the local QCD sum rule for a_2, which favors a large positive $a_2 \sim 0.4$. One explanation for the failure of the corresponding QCD sum rule could be that already the case $n = 2$ may be too "nonlocal" for sum rules to work. Another one could be that the treatment of a_1 and other resonances contributing to that sum rule may be insufficient. We leave a further discussion of that question to future work. The result from sum rules with nonlocal condensates [24,25,31], shown as a black square in Fig. 2, is also outside the favored area in Fig. 2, which is mainly due to the large value of $|a_4|$. It would definitely be very interesting to see all these results and constraints on $a_{2,4}$ be supplemented by lattice determinations.

The only parameter left to discuss is a_1 for the K meson (by which we understand an $s\bar{q}$ bound state), which is a G-parity breaking parameter. Here the situation is even worse than for $a_{2,4}$, as neither size nor even sign of that quantity are reliably known. The facts at hand are the following: the intuitive expectation is that a_1 (i.e., the moment with a weight function proportional to $2u - 1$) should be positive, as the DA is expected to be slightly tilted towards larger values of u which is the momentum fraction carried by the (heavier) s quark in the meson—the heavier the quark, the more the DA is expected to peak at large u, the extreme case being a $b\bar{q}$ bound state whose DA should be close to $\delta(1 - u)$. The (tree-level) QCD sum rule calculation in [22] seemed to confirm intuition, but was challenged, when Ref. [33] found a sign mistake in that calculation and, including two-loop radiative corrections, obtained a *negative* sign for a_1^K. For this paper, we first decided to stick to that result and use the central value $a_1^K(1\text{ GeV}) = -0.18$. It turned out, however, that this value tends to produce form factors with an unfavorable q^2 dependence.[8] We therefore decided to revert to the original result by CZ [22] and use

$$a_1^K(1\text{ GeV}) = 0.17 \leftrightarrow a_1^K(2.2\text{ GeV}) = 0.135. \qquad (25)$$

The conclusion from that inconclusive situation can only be that a second opinion has to be sought, and we urge our colleagues from the lattice community to take up the challenge and provide the first-ever lattice determination of a_1^K. For the time being, we will present our results in a way that makes it possible to obtain the form factors also for different values of a_1^K.

[8]That is, the form factors are not very compatible with the parametrization discussed in Sec. IV D, which is based on generic analytic properties of the form factors.

C. Results for $q^2 = 0$

Let us first discuss the sum rule results for $q^2 = 0$. They are collected in Table I, for all four parameter sets from Table III.[9] Including the uncertainty of m_b, $m_b = (4.80 \pm 0.05)$ GeV, the final central values and uncertainties of the form factors are given in Eq. (27).

The form factors are calculated from Eq. (16) using the parameter sets given in Table III and the hadronic input parameters given in Eqs. (24) and (25) and Table IV. The dependence of the form factors on m_b, i.e., the set, is shown in Fig. 3. It is evident that the residual dependence of $f(0)$ on m_b is much smaller than the one of f_B in Table I, which confirms our expectation that the calculation of f_B from a sum rule reduces the parameter dependence of the form factors. $f_+^\pi(0)$ depends sensitively on a_2 and a_4 as illustrated in Fig. 4. The form factors show moderate SU(3) breaking between π and η, which is due to terms in the LCSRs proportional to the meson mass. For K, the situation is different, and we observe a strong enhancement of the form factor due to the combination of two effects: the fact that f_K is larger than f_π and the positive contribution of the Gegenbauer moment a_1 to the form factor. As discussed in the previous subsection, the numerical value of a_1, and even its sign, is not precisely known. Figure 5(a) illustrates the dependence of $f_+^K(0)$ on a_1, which is quite strong. Figure 5(b) shows the dependence of $f_+^K(q^2)$ on q^2 for different values of a_1. It is evident that a_1 mainly determines the normalization of the form factor, but has only minor impact on its shape. The uncertainty of $f_+^K(0)$ induced by a_1 will be discussed below. The dependence of $f_+^\pi(0)$ on the sum rule parameters M^2 and s_0 is illustrated in Fig. 6 and is very mild, thanks to the optimized criteria for choosing M^2 and s_0 outlined in Sec. IVA. The behavior of the other form factors is very similar. In Fig. 7 we show the variation of $f_+^\pi(0)$ with a change of the factorization scale $\mu_{\rm IR}$ in the large range 1 GeV $\leq \mu_{\rm IR} \leq m_b$. The curve is remarkably flat which can be understood from the fact that radiative corrections cancel to a certain extent between Π_+ and f_B and that large logarithms of type $\ln m_b/\mu_{\rm IR}$ occur only at subleading order in the conformal expansion of the DAs, which is numerically suppressed with respect to the leading ($\mu_{\rm IR}$-independent) term, and at subleading twist, which is also suppressed.

Let us now turn to the uncertainties of the form factors induced by a variation of the input parameters. It is convenient to split the form factors into contributions from different Gegenbauer moments,

$$f(q^2) = f^{as}(q^2) + a_1 f^{a_1}(q^2) + \{a_2 f^{a_2}(q^2) + a_4 f^{a_4}(q^2)\}, \qquad (26)$$

where f^{as} contains the contributions to the form factors from the asymptotic DA and also all higher-twist effects

[9]$f_0(0)$ is not included as $f_0(0) \equiv f_+(0)$.

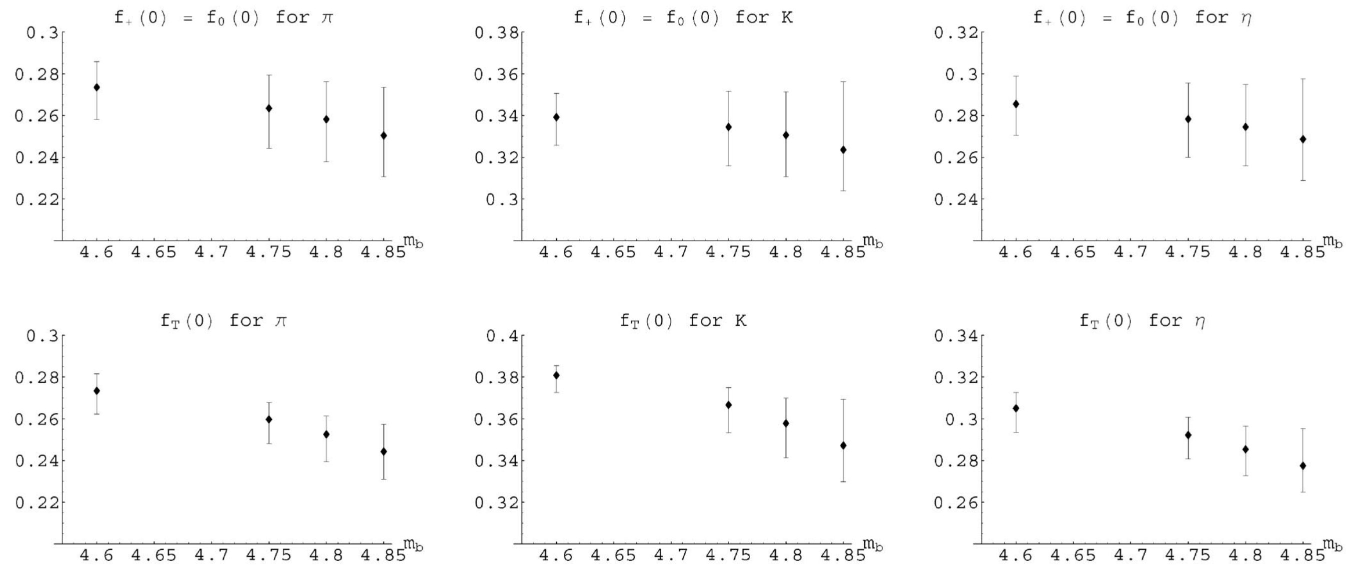

FIG. 3. Central values of the form factors $f(0)$ and uncertainties Δ. Numbers are from Table I.

from three-particle quark-quark-gluon matrix elements. Explicit expressions for the functions f^{as,a_1,a_2,a_4} can be obtained from Table V; in particular $f^{a_i}(0)$ is just given by the parameters a in that table. We calculate separately the uncertainties Δ_{as,a_1} of the first and second term and the combined uncertainty Δ_{a_2,a_4} of the term in curly brackets. We start with Δ_{as}. To estimate its value we vary the following quantities:

(i) the threshold s_0 by ± 0.5 GeV^2;
(ii) the Borel parameter M^2 in Eq. (19) by ± 1.2 GeV^2;
(iii) the infrared factorization scale $\mu_{\rm IR}^2 = m_B^2 - m_b^2$ by ± 2 GeV^2;
(iv) the quark condensate and the mixed condensate as indicated in Eq. (18);
(v) the twist-3 matrix element η_3 by $\pm 50\%$.

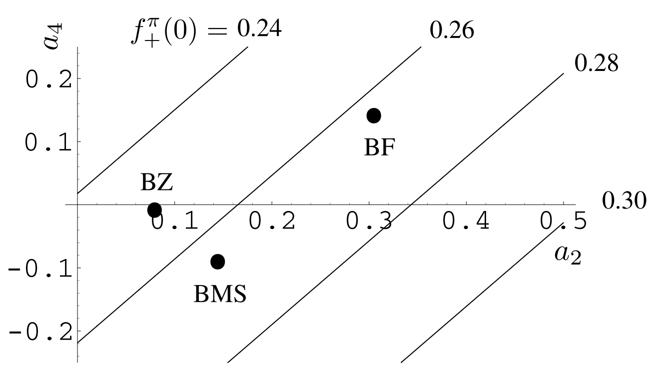

FIG. 4. Dependence of $f_+^\pi(0)$ on $a_2(\mu_{\rm IR})$ and $a_4(\mu_{\rm IR})$, for parameter set 2. The lines are lines of constant $f_+^\pi(0)$. The dot labeled BZ denotes our preferred values of $a_{2,4}$, BMS the values from the nonlocal-condensate model, and BF the values from the sum rule calculations of Ref. [16].

m_b is kept fixed and we calculate the uncertainty separately for each parameter set; for a given form factor, Δ_{as} is then the largest uncertainty of the four sets. The errors are correlated and we therefore scan the five-parameter

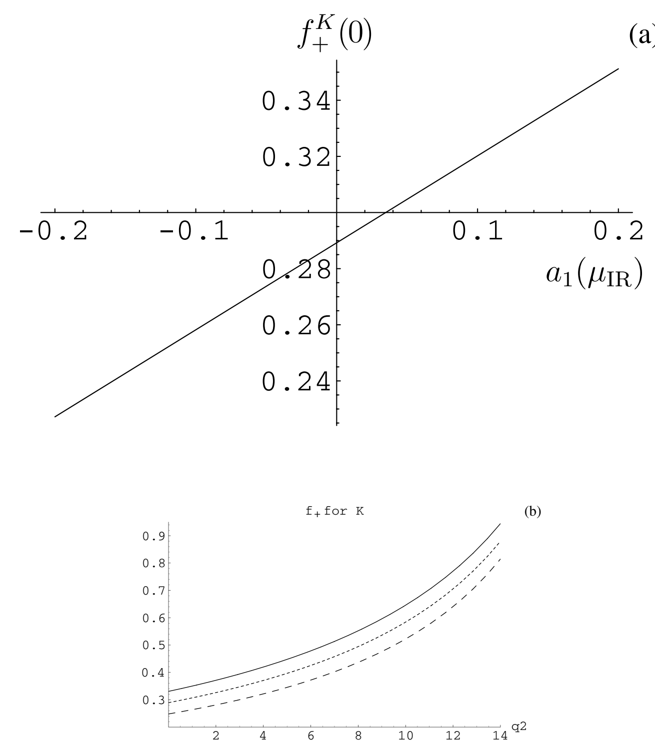

FIG. 5. (a) Dependence of $f_+^K(0)$ on the Gegenbauer moment $a_1(\mu_{\rm IR})$. (b) $f_+^K(q^2)$ as function of q^2 for different values of a_1. Solid line: $a_1^K(1\ {\rm GeV}) = 0.17$; short dashes: $a_1^K(1\ {\rm GeV}) = 0$; long dashes: $a_1^K(1\ {\rm GeV}) = -0.18$. Input parameters: set 2.

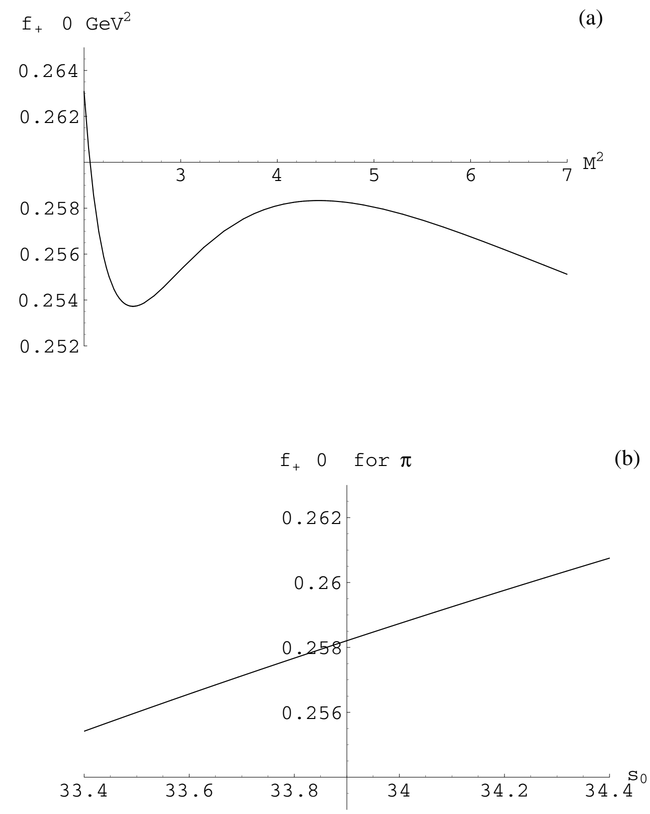

FIG. 6. Dependence of $f_+^\pi(0)$ on (a) the Borel parameter M^2 and (b) the continuum threshold s_0. Input parameters: set 2 in Table III.

space for the largest deviations from the central values. The resulting Δ_{as} are given in Table I.

The uncertainty of $f^K(0)$ induced by a_1 is dominated by a_1 itself, so we do not attempt to determine the uncertainty of f^{a_1} arising from varying M^2, s_0, etc., but just take the maximum value of $f^{a_1}(0) \equiv a$ from Table V and multiply it by $\delta_1 = a_1(1\text{ GeV}) - 0.17$ and the

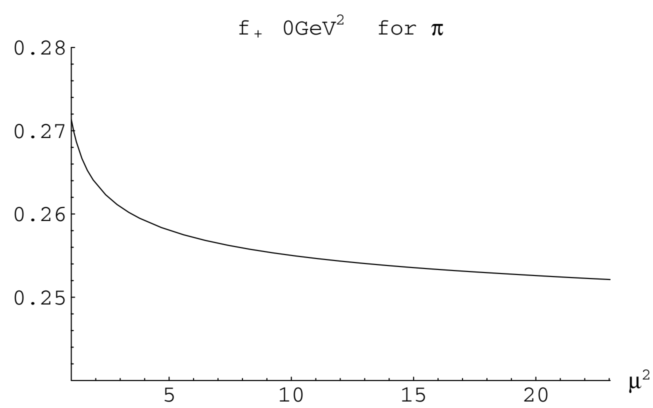

FIG. 7. Dependence of $f_+^\pi(0)$ on the factorization scale μ_{IR}. Same input parameters as in Fig. 6.

leading-order scaling factor from 1 GeV to μ_{IR}, which gives the entry labeled Δ_{a_1} in Table I.

As the allowed input values of a_2 and a_4 are correlated and given by the rhomboid shown in Fig. 2, we only determine the combined uncertainty Δ_{a_2,a_4} arising from the corresponding variation of the Gegenbauer moments, separately for each parameter set. The resulting uncertainties depend strongly on the precise values of M^2 and s_0, so for a conservative estimate of the uncertainty we scan the full seven-parameter space in a_2, a_4, M^2, etc. and quote the largest deviation from the central value as uncertainty, which yields the Δ_{a_2,a_4} quoted in Table I. Taking everything together, and including the variation of $m_b = (4.80 \pm 0.05)$ GeV in the error estimate, adding errors in quadrature, we find (δ_{a_1} is defined in Table I):

$$\begin{aligned} f_+^\pi(0) &= 0.258 \pm 0.031, \qquad f_T^\pi(0) = 0.253 \pm 0.028, \\ f_+^K(0) &= 0.331 \pm 0.041 + 0.25\delta_{a_1}, \\ f_T^K(0) &= 0.358 \pm 0.037 + 0.31\delta_{a_1}, \\ f_+^\eta(0) &= 0.275 \pm 0.036, \qquad f_T^\eta(0) = 0.285 \pm 0.029. \end{aligned} \tag{27}$$

These are our final results for the form factors at $q^2 = 0$. For $f^{\pi,\eta}$ the total theoretical uncertainty is 10% to 13%, for f^K it is 12%, plus the uncertainty in a_1, which hopefully will be clarified through an independent calculation in the not too far future. These uncertainties include a variation of both the external input parameters and the sum rule specific parameters, but they do not include an additional "systematic" uncertainty of the sum rule method itself. To a certain extent, this intrinsic sum rule uncertainty is included by the variation of the sum rule specific parameters M^2 and s_0, which sets the minimum uncertainty of the result: all external hadronic parameters fixed, this variation induces a $\sim$7% uncertainty of $f_+^\pi(0)$ quoted in Eq. (27). Realistically, one may hope to reduce the $\sim$12% uncertainty quoted to $\sim$10% by reducing the errors on the Gegenbauer moments $a_{2,4}$ by a factor of 2. Further improvement will then have to come from a better control over higher-twist matrix elements, dominated by the quark condensate and the quark-quark-gluon matrix element η_3 discussed in App. B.

D. Results for $q^2 \neq 0$, Fits and Extrapolations

In this subsection we calculate the q^2 dependence of the form factors for central values of the input parameters and cast them into a three-parameter parametrization that is valid for all q^2. The results are given in Table II which is to be used together with Eq. (30). The fit parameters for other sets of input parameters are given in App. A. We refrain from a complete analysis of the uncertainty of the q^2 dependence of the form factors, but just mention that it is likely to be smaller than that at $q^2 = 0$, which is indicated by a decrease of the spread between the form factors calculated from the different parameter sets in Table III cf. Fig. 8.

TABLE V. Fit parameters for Eq. (A6) for the functions f^{a_i} defined in (A5). δ is a measure of the quality of the fit and is defined in (A7).

	set 2, $m_b = 4.8$ GeV					set 4, $m_b = 4.6$ GeV				
	a	$b \times 10^2$	$c \times 10^2$	$d \times 10^3$	δ	a	$b \times 10^2$	$c \times 10^2$	$d \times 10^3$	δ
$f_+^K(a_1)$	0.310	0.930	0.139	−0.083	0.3	0.276	0.060	0.151	−0.157	0.7
$f_0^K(a_1)$	0.308	0.106	0.026	−0.048	0.2	0.273	−0.433	0.0001	−0.051	0.2
$f_T^K(a_1)$	0.381	1.056	0.167	−0.108	0.3	0.354	0.027	0.178	−0.194	0.7
$f_+^\pi(a_2)$	0.187	−0.517	0.014	−0.117	0.5	0.040	−0.762	−0.201	0.050	1.5
$f_0^\pi(a_2)$	0.185	−0.841	− 0.075	−0.005	0.4	0.041	−1.078	−0.123	0.068	1.2
$f_T^\pi(a_2)$	0.203	−0.659	− 0.008	−0.118	0.3	0.038	−0.944	−0.244	0.073	1.5
$f_+^K(a_2)$	0.228	−0.632	0.017	-0.143	0.5	0.049	−0.931	−0.245	0.061	1.5
$f_0^K(a_2)$	0.226	−1.031	− 0.092	−0.005	0.4	0.050	− 1.32	−0.150	0.083	1.2
$f_T^K(a_2)$	0.264	−0.858	− 0.011	−0.153	0.3	0.049	−1.228	−0.318	0.095	1.5
$f_+^\eta(a_2)$	0.185	−0.514	0.014	−0.116	0.5	0.039	−0.757	−0.199	0.049	1.5
$f_0^\eta(a_2)$	0.183	−0.829	− 0.076	−0.002	0.4	0.041	−1.068	-0.122	0.069	1.2
$f_T^\eta(a_2)$	0.216	−0.722	− 0.007	−0.128	0.3	0.040	−1.019	−0.259	0.076	1.4
$f_+^\pi(a_4)$	− 0.141	−0.775	0.004	0.161	0.7	−0.054	−0.506	0.621	−0.326	5.2
$f_0^\pi(a_4)$	− 0.139	−0.687	0.170	0.002	1.5	−0.061	0.703	0.323	−0.209	2.9
$f_T^\pi(a_4)$	− 0.167	−0.895	0.077	0.143	1.1	−0.047	−0.327	0.698	−0.394	4.9
$f_+^K(a_4)$	− 0.173	−0.947	0.005	0.196	0.7	−0.067	−0.618	0.759	−0.398	5.2
$f_0^K(a_4)$	− 0.170	−0.838	0.209	0.001	1.5	−0.075	0.871	0.392	-0.254	2.9
$f_T^K(a_4)$	− 0.217	−1.165	0.101	0.187	1.1	−0.061	−0.426	0.909	−0.513	4.9
$f_+^\eta(a_4)$	− 0.140	−0.770	0.004	0.159	0.7	−0.054	−0.502	0.616	−0.323	5.2
$f_0^\eta(a_4)$	− 0.138	−0.681	0.170	0.0005	1.5	−0.061	0.710	0.318	−0.206	2.9
$f_T^\eta(a_4)$	− 0.178	−0.955	0.083	0.153	1.1	−0.050	−0.349	0.745	−0.421	4.9

The validity of the LCSR approach is restricted to the kinematical regime of large meson energies, $E_P \gg \Lambda_{\rm QCD}$, which via the relation

$$q^2 = m_B^2 - 2m_B E_P$$

implies a restriction to small and moderate q^2; specifically, we evaluate the sum rules only for $0 \leq q^2 \leq 14\ \mathrm{GeV}^2$. The resulting form factors are plotted in

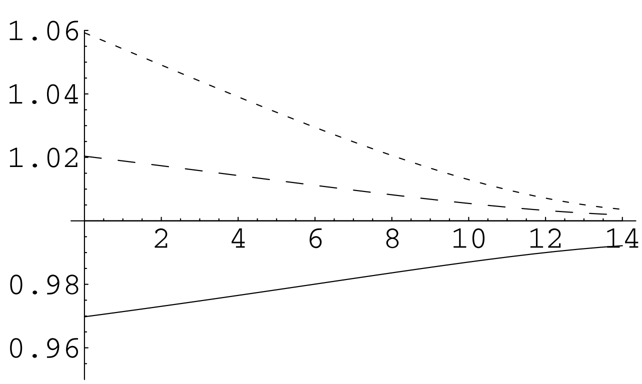

FIG. 8. Ratio of $f_+^{\pi(\mathrm{set}i)}(q^2)/f_+^{\pi(\mathrm{set}2)}(q^2)$ as function of q^2. Solid line: set 1; long dashes: set 3; short dashes: set 4.

Fig. 9, using the parameter set 2 in Table III and the hadronic input parameters given in Eqs. (24) and (25) and Table IV. As expected from LEET [34], f_+ and f_T nearly coincide. Although this agreement is expected to be best for small q^2, i.e., large energies of the light meson, it is seen to hold for all q^2. From the LCSR point of view, this agreement is due to the fact that the leading twist-2 contributions to the corresponding correlation functions coincide at tree level. The figure also shows that the q^2 dependence of f_0 is weaker than that of the other form factors. This can be understood from the fact that, if f_+ is represented as a dispersion relation over hadronic states, these states have quantum numbers $J^P = 1^-$ and hence zero orbital angular momentum, whereas for f_0 the quantum number is $J^P = 0^+$ and thus the coupling of these states or, in the language of potential models, their wave function at the origin, is suppressed as it corresponds to a state with orbital angular momentum $L = 1$. Figure 9 also shows sizable SU(3) breaking for the K, but a moderate one for η, which is due to the same effects discussed for the form factors at $q^2 = 0$. In Fig. 8 we show $f_+^\pi(q^2)$ as function of q^2, calculated for sets 1, 3, and 4 and normalized to set 2. It is evident that the uncertainties induced by m_b, which amount to 6% at $q^2 = 0$, become less impor-

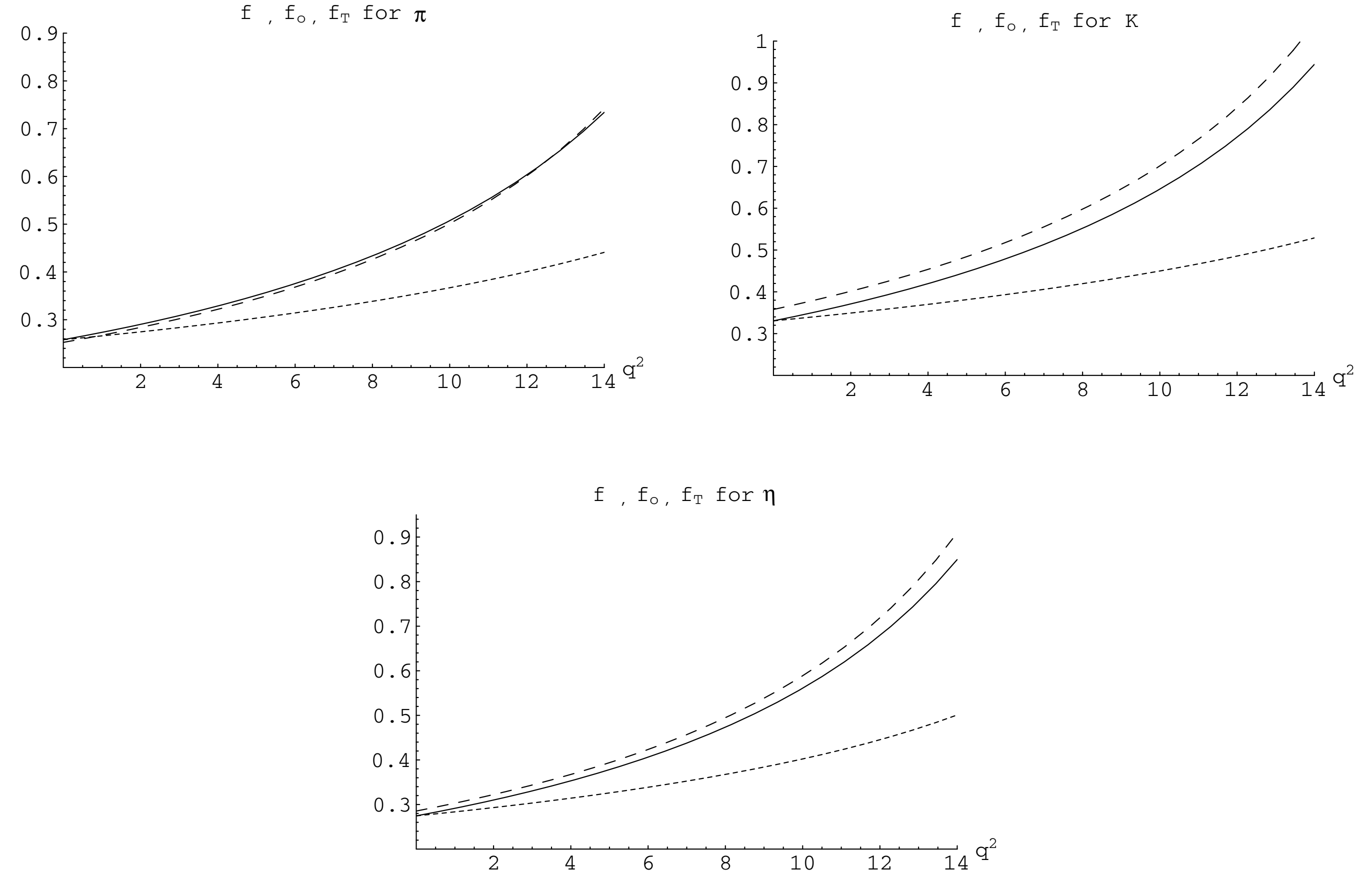

FIG. 9. f_+ (solid lines), f_0 (short dashes) and f_T (long dashes) as functions of q^2 for π, K, and η. The renormalization scale of f_T is chosen to be m_b. Input parameters: set 2 in Table III.

tant for larger q^2, so that for instance the branching ratio of the semileptonic decay $B \to \pi e \nu$ will be less dependent on the precise value of m_b than $f_+^\pi(0)$.

One of the main goals of this paper is to give simple expressions for the form factors in the full physical regime $0 \leq q^2 \leq (m_B - m_P)^2 \approx 23\ \mathrm{GeV}^2$. We thus have to find a parametrization that

(i) reproduces the data below $14\ \mathrm{GeV}^2$ with good accuracy;

(ii) provides an extrapolation to $q^2 > 14\ \mathrm{GeV}^2$ that is consistent with the expected analytical properties of the form factors and reproduces the lowest-lying resonance (pole) with $J^P = 1^-$ for f_+ and f_T.[10]

It is actually not very difficult to find good fits: the parametrization

$$f(q^2) = \frac{f(0)}{1 - a_F q^2/m_B^2 - b_F(q^2/m_B^2)^2} \qquad (28)$$

advocated in previous works, e.g. [4], is one example for an excellent fit to the results of the sum rules for $q^2 < 14\ \mathrm{GeV}^2$. In the present context, however, it turns out to be unsuitable as it produces, for f_+^π, a pole at $q^2 \approx 23\ \mathrm{GeV}^2$, which is below the physical pole at $q^2 = m_{B^*}^2 = (5.32\ \mathrm{GeV})^2$. In our previous paper [4] we argued that the above parametrization should be matched to a simple pole-dominance formula $f_+ \sim 1/(m_{B^*}^2 - q^2)$ for q^2 above a certain threshold $q_0^2 \sim 15\ \mathrm{GeV}^2$, defined as the value of q^2 that would allow a smooth transition[11] from one parametrization to the other. This procedure unfortunately does not work for our new form factors, as the optimum q_0^2 turns out to be far outside the physical regime. We therefore decide to follow, as far as possible, the procedure advocated by Becirevic and Kaidalov [35], who suggested to write the form factor f_+ as a dispersion relation in q^2 with a lowest-lying pole plus a contribution from multiparticle states, which in turn is to be replaced by an effective pole at higher mass:

[10]For f_0, the lowest pole with quantum numbers 0^+ lies above the two-particle threshold starting at $(m_B + m_P)^2$ and hence is not expected to feature prominently.

[11]That is equality of both the parametrization formulas and their first derivatives in q_0^2.

$$f_+(q^2) = \frac{r_1}{1-q^2/m_1^2} + \int_{(m_B+m_P)^2}^{\infty} ds \frac{\rho(s)}{s-q^2} \tag{29}$$

$$\to \frac{r_1}{1-q^2/m_1^2} + \frac{r_2}{1-q^2/m_{\rm fit}^2}. \tag{30}$$

The lowest-lying resonance in the $b\bar{u}$ channel is well-known experimentally: it is the $B^*(1^-)$ vector meson with mass 5.32 GeV; this is also the mass to be used for the η, as the $B \to \eta$ form factors calculated in this paper refer to a $b \to u$ transition. For the K we have calculated the mass of the B_s^* resonance in the heavy-quark limit and find

$$m_{B_s^*}^2 - m_{B_s}^2 = m_{B^*}^2 - m_B^2 \quad \longrightarrow \quad m_1^K = m_{B_s^*} = 5.41 \text{ GeV}.$$

For Eq. (30) to describe all f_+ and also f_T, which feature the same 1^- resonance, in terms of three fit parameters, r_1, r_2, and $m_{\rm fit}$, it is crucial that the position of the lowest pole is sufficiently below the two-particle cut starting at $(m_B + m_P)^2$. We find that indeed most $f_{+,T}^\pi$ form factors, with the exception of $f_T^{\pi(\text{set } 4)}$, are described very well by (30). For $f_T^{\pi(\text{set } 4)}$, however, and all $f_{+,T}^{K,\eta}$, $m_{\rm fit}$ gets too close to m_1, so that the fit becomes numerically unstable. In this case, it is appropriate to expand (30) to first order in $m_{\rm fit} - m_1$, which yields

$$f_{+,T}^{K,\eta}(q^2) = \frac{r_1}{1-q^2/m_1^2} + \frac{r_2}{(1-q^2/m_1^2)^2} \tag{31}$$

with fit parameters r_1 and r_2, and $m_1 = m_{B^*,B_s^*}$ fixed.

For f_0, one can write a decomposition similar to (29), but here the lowest-lying pole with quantum numbers 0^+ lies either above the two-particle threshold (for π and η) or is very close to it (for K cf. Table VI), so that the pole is effectively hidden under the cut and only the dispersive term survives in (29). We again follow the suggestion of Becirevic and Kaidalov and replace this term by an effective pole, i.e., we set

$$f_0(q^2) = \frac{r_2}{1-q^2/m_{\rm fit}^2}. \tag{32}$$

The accuracy of the fits of the LCSR results to the above parametrizations is generally very high and best for sets 1 to 3 of Table III with $m_b = (4.80 \pm 0.05)$ GeV, with a maximum 1.2% deviation; set 4 fares slightly worse with an accuracy of 2% or better. The quality of the fits is discussed in more detail in App. A. The uncertainty introduced by fitting is much smaller than the actual uncertainty of the sum rule calculation, which we have found to be around 10% at $q^2 = 0$, and also much smaller than the intrinsic and irreducible sum rule uncertainty, which we have estimated to be $\sim$7%. Nevertheless it is legitimate to ask whether the extrapolation of the fits to $q^2 > 14$ GeV^2, or the variation of the "cutoff" $q^2_{\rm max} = 14$ GeV^2, introduce an additional uncertainty. In answering this question, we first would like to recall that for most applications it is actually sufficient to know the form factors for $q^2 < 14$ GeV^2 only—these include, in particular, nonleptonic B decays treated in QCD factorization, and also the rare decays $B \to (\pi, K, \eta)\ell^+\ell^-$, as the spectrum for invariant lepton masses above the $c\bar{c}$ threshold, i.e., $q^2 \geq m_{J/\psi}^2 \approx 10$ GeV^2, is dominated by long-distance processes unrelated to $B \to (\pi, K, \eta)$ form factors. The only, but very important case where the form factor is needed over the full range of q^2 is the semileptonic decay $B \to \pi\ell\nu$, which depends on f_+^π and (for decays into τ) on f_0^π. We discuss the effect of the extrapolation on this decay by studying three different parametrizations of f_+^π:

fit 1 Equation (30), our standard parametrization;

fit 2 a modified version of (28), with one zero of the denominator fixed at $m_1^2 = m_{B^*}^2$:

$$f_+^\pi(q^2) = \frac{f_+^\pi(0)}{(1-q^2/m_1^2)(1-q^2/m_{\rm fit}^2)};$$

fit 3 a parametrization similar to (31), but with the pole mass as fit parameter:

$$f_+^\pi(q^2) = \frac{r_1}{1-q^2/m_{\rm fit}^2} + \frac{r_2}{(1-q^2/m_{\rm fit}^2)^2}.$$

We quantify the difference between these parametrizations by calculating the semileptonic decay rate, the integral of Eq. (4) over q^2 from 0 to $(m_B - m_\pi)^2$, normalizing to our central values, set 2 and fit 1. The results are collected in Table VII. It is evident that the dependence of the rate on the fit is rather mild, despite the double-pole of fit 3, which is however sufficiently far away from the end point of the spectrum, $m_{\rm fit} = (5.6 \pm 0.1)$ GeV, and hence

TABLE VI. Masses of 1^- and 0^+ resonances in the $b\bar{u}$ and $b\bar{s}$ channels. The 1^- masses are obtained from experiment and heavy-quark relations, the 0^+ masses from a potential model [36]. All numbers are in units GeV^2.

	m_1^2 (1^-)	m_{1*}^2 (0^+)	$q^2_{\rm max}$
$\pi(\eta)$	$5.32^2 = 28.4$	$5.63^2 = 31.7$	26.4 (22.8)
K	$5.41^2 = 29.3$	$5.72^2 = 32.7$	23.8

TABLE VII. Total semileptonic decay rates $\Gamma(B \to \pi e\nu)$ normalized to 1 for set 2, fit 1, for different form factor parametrizations and input parameter sets.

	set 1	set 2	set 3	set 4
fit 1	0.97	1	1.01	1.05
fit 2	0.97	0.98	0.99	1.00
fit 3	0.95	0.98	1.00	1.04

has only moderate impact on the rate. We conclude that the extrapolation of f_+^π causes an uncertainty in the total semileptonic decay rate $\Gamma(B \to \pi e\nu)$ which is considerably less than the expected intrinsic sum rule uncertainty of $\sim$14%.

We conclude the discussion of the uncertainty of the extrapolations by studying the effect of changing the maximum value of q^2 for which the sum rules results are included in the fits. Our default value $q^2_{\rm max}$ is 14 GeV^2; lowering $q^2_{\rm max}$ changes the fit parameters of all three parametrizations and hence the predictions for the total semileptonic decay rate. Figure 10 shows the corresponding change in the rate, normalized to our central values fit 1 and $q^2_{\rm max} = 14$ GeV^2. Again the dependence of the rate on $q^2_{\rm max}$ is mild, which corroborates our conclusion that the precise shape of the form factor is not that relevant, as long as it does not exhibit too strong a singularity at $q^2 = (5.32\ \text{GeV})^2$.

There are also other tests and checks for the validity of the extrapolation of (30) to the full physical regime $q^2 < (m_B - m_P)^2$: first, the coefficient r_1 for f_+^π is related to the coupling $g_{BB^*\pi}$ as

$$r_1 = \frac{f_{B^*} g_{BB^*\pi}}{2m_{B^*}}. \tag{33}$$

At the upper end of the physical range in q^2 we can expect vector-meson dominance to be effective and therefore the fit parameter should be close to the above value. In fact lattice [37] and meson-loop calculations (cf. Ref. 1 in [6]) yield $r_1 \approx 0.8$, but are at variance with a determination of $g_{BB^*\pi}$ from LCSRs which yields $r_1 \approx 0.44$ [5]. The lattice and meson-loop calculations are further supported by the agreement of their predictions for $g_{DD^*\pi}$ with experimental measurements, whereas LCSRs again give a value that is too low by almost a factor of 2. The author of Ref. [38] speculates that this discrepancy might be due to a failure of the simple quark-hadron duality ansatz used for the contribution of higher resonances and the continuum to the sum rules. Ref. [39] demonstrates that this suggestion does indeed point into the right direction: the inclusion of a radial excitation with negative residue in the hadronic parametrization of the correlation function does increase the value of r_1.[12] If we interpret our fit results as determinations of $g_{BB^*\pi}$, we get the following values of r_1 for the sets 1 to 4: (0.73,0.74,0.77,0.94) (cf. Table VIII), which is in reasonable agreement with lattice and meson-loop calculations.

Second, there is one further constraint on the form factor f_0. As first pointed out in Ref. [40], in the soft-pion limit $p \to 0$ and $m_\pi^2 \to 0$ (i.e., $q^2 = m_B^2$) $f_0^\pi(m_B^2)$ is related to the decay constants of the B and π as

[12] Note that the corresponding spectral function is not positive definite.

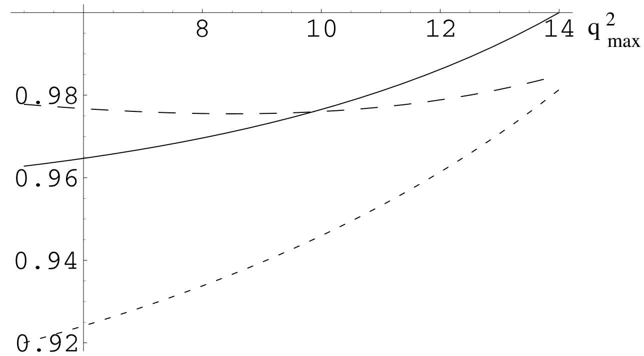

FIG. 10. Variation of the total semileptonic rate $\Gamma(B \to \pi e\nu)$ as function of $q^2_{\rm max}$, the maximum q^2 for which LCSR results are included in the fits. The rate is normalized to 1 for $q^2_{\rm max} = 14$ GeV^2 and fit 1. Solid line: fit 1; long dashes: fit 2; short dashes: fit 3. Input parameters: set 2.

$$f_0^\pi(m_B^2) = \frac{f_B}{f_\pi}. \tag{34}$$

We can compare this relation with our parametrization by solving it for f_B. For the four parameter sets of Table III, we get from Eq. (34) $f_B^{\rm set1} = 201$ MeV, $f_B^{\rm set2} = 193$ MeV, $f_B^{\rm set3} = 190$ MeV, and $f_B^{\rm set4} = 207$ MeV, which is in good agreement with lattice and sum rule calculations.

Let us conclude with one more remark. In LEET, f_+ and f_0 are related as [34]:

$$f_0 = \frac{2E}{m_B} f_+, \tag{35}$$

which is valid in the combined limits $m_B \to \infty$ and $E \to \infty$. This constraint was used in Ref. [35] to reduce the number of fit parameters to two as necessitated by the limited accuracy of the lattice form factors. We do not impose this constraint explicitly, but find that it is valid to 4% accuracy for our form factors, for not too large q^2.

Summarizing, we conclude that, for all form factors, the three-parameter formula (30) provides both an excellent fit to the LCSR results for $q^2 < 14$ GeV^2 and a smooth extrapolation to $14\ \text{GeV}^2 < q^2 < (m_B - m_P)^2$, and is consistent with all known constraints.

V. SUMMARY & CONCLUSIONS

In this paper we have given a thorough and careful examination of the predictions of QCD sum rules on the light-cone for the form factors f_+, f_0, and f_T for the decays $B \to \pi, K, \eta$. We have not discussed $B \to \eta'$, which is not accessible within the method due to its large mass.

The main improvements of our results with respect to our previous publications [3,4] are:

TABLE VIII. Fit parameters for the π Eq. (A1) for both the full form factors and the asymptotic ones, f^{as}, Eq. (A5), using the sets 2 and 4 in Table III. The form factor f_0 is fitted to the parametrization (A3). The mass parameters m_1^x are given in Table VI. Δ is a measure of the quality of the fit and is defined in (A4).

	set 2, $m_b = 4.8$ GeV					set 4, $m_b = 4.6$ GeV				
	r_1	m_1^2	r_2	$m_{\rm fit}^2$	Δ	r_1	m_1	r_2	$m_{\rm fit}^2$	Δ
f_+^π	0.744	$(m_1^\pi)^2$	-0.486	40.73	0.3	0.944	$(m_1^\pi)^2$	− 0.669	34.27	0.3
f_0^π	0	—	0.258	33.81	0.1	0	—	0.270	33.63	1.2
f_T^π	1.387	$(m_1^\pi)^2$	− 1.134	32.22	0.5	use (A2) with $r_1 = 0.152$, $r_2 = 0.122, m_1 = m_1^\pi, \Delta = 0.4$				
$f_+^{\pi,as}$	0.918	$(m_1^\pi)^2$	− 0.675	38.20	0.1	0.711	$(m_1^\pi)^2$	− 0.441	44.31	0.1
$f_0^{\pi,as}$	0	—	0.244	30.46	0.8	0	—	0.270	31.93	0.1
$f_T^{\pi,as}$	1.556	$(m_1^\pi)^2$	− 1.321	32.56	0.2	1.331	$(m_1^\pi)^2$	− 1.061	33.43	0.4

(i) predictions for all form factors of $B \to \pi, K, \eta$ transitions to $O(\alpha_s)$ accuracy for twist-2 and -3 two-particle contributions;
(ii) a well-defined and precise method for fixing sum rule specific parameters (cf. Sec. IVA);
(iii) a careful assessment of uncertainties at zero momentum transfer (cf. Sec. IV B and IV C);
(iv) a detailed breakdown of the contributions of different Gegenbauer moments a_i to the form factors (cf. App. A), which
  (a) renders straightforward the implementation of future updates of these parameters;
  (b) allows the assessment of the impact of nonasymptotic twist-2 distribution amplitudes on QCD factorized nonleptonic B decays in a coherent way, to 4th order in the conformal expansion;
(v) a parametrization of the q^2 dependence of form factors valid in the full physical regime of momentum transfer that reproduces all relevant analytical properties of the form factors (cf. Sec. IV D).

Our main results for $q^2 = 0$ are collected in Table I and Eq. (27). They depend crucially on the values of the Gegenbauer moments describing the twist-2 distribution amplitudes of π, K, and η cf. App. B. We have determined these parameters as discussed in Sec. IVA, but a better determination from an independent source, e.g., lattice calculations, would be extremely useful. This applies, in particular, to the SU(3) breaking parameter a_1^K, whose size and even sign is under discussion (cf. Ref. [33]). Once more precise values for these parameters will be available, it is straightforward to obtain the corresponding form factors from the data collected in App. A. Setting aside a_1, the total theoretical uncertainty of the form factors at $q^2 = 0$ is 10% to 13%, which includes a variation of all input parameters. It can be further improved by reducing the uncertainties of, in particular, a_2, a_4, the quark condensate, and η_3, the dominant quark-quark-gluon matrix element. A reduction of the uncertainty of $a_{2,4}$ by a factor of 2 will give a $\sim$2% gain in accuracy, reducing the uncertainty of the quark condensate and η_3 by the same factor will give another 2%. The uncertainty due to the variation of only the sum rule specific parameters is 7%, which cannot be reduced any further and hence sets the minimum theoretical uncertainty that can be achieved within this method. Comparing with the uncertainties quoted in our previous publications, we have achieved a reduction of the global estimate $\sim$15% quoted in [3] and also of the 20% uncertainty for $f_+^\pi(0)$ quoted in [4]. This is partially due to a reduction of the uncertainties of the hadronic input parameters, in particular m_b, and partially due to a refinement of the assessment of sum rule specific uncertainties as discussed in Sec. IVA.

We have also calculated all form factors for $0 \leq q^2 \leq 14$ GeV^2; the upper bound on q^2 is due to the limitations of the light-cone expansion which requires the final-state meson to have energies $E \gg \Lambda_{\rm QCD}$: for $q^2_{\rm max} = 14$ GeV^2 the meson energy is $E = 1.3$ GeV. In order to allow a simple implementation of our results, we have given a parametrization that includes the main features of the analytical properties of the form factors and is valid in the full physical regime $0 \leq q^2 \leq (m_B - m_P)^2$. The corresponding results for our preferred set of input parameters are given in Table II; a detailed breakdown of the contributions of different parameters to the full form factors is given in App. A. The main features of the results are that the form factors f_+ and f_T are nearly equal as predicted by LEET and that f_0 is very well described by a single-pole formula. The uncertainty induced by the extrapolation of the parametrization to larger momentum transfers is an issue only for the semileptonic decay $B \to \pi e \nu$; we have checked that the change of the total rate is at most 5% for three different extrapolations of the light-cone sum rule results.

Our approach is complementary to standard lattice calculations, in the sense that it works best for large energies of the final-state meson (i.e., small q^2), whereas lattice calculations work best for small energies—a situation that may change in the future with the implementation of moving NRQCD [10]. Previously, the LCSR results for $f^\pi_{+,0}$ at small and moderate q^2 were found to nicely match the lattice results obtained for large q^2 [41]. The situation will have to be reassessed in view of our new results and it will be very interesting to see if and how it will develop with further progress in both lattice and LCSR calculations.

ACKNOWLEDGMENTS

R. Z. is grateful to M. B. Voloshin for clarifications and to W. Jaus for calling his attention to the CLEO measurement of $g_{DD^*\pi}$; he is supported by the Swiss National Science Foundation. P. B. would like to thank the W. I. Fine Theoretical Physics Institute at the University of Minnesota in Minneapolis for hospitality while this paper was semi-finalized.

APPENDIX A: FIT PARAMETERS AND COMMENTS

This appendix extends the discussion of Sec. IV D.

1. Full form factors

As discussed in Sec. IV D, we fit the LCSR results to the following parametrizations:

(i) for $f^\pi_{+,T}$:[13]

$$f(q^2) = \frac{r_1}{1 - q^2/m_1^2} + \frac{r_2}{1 - q^2/m_{\rm fit}^2}, \tag{A1}$$

where m_1^π is the mass of $B^*(1^-)$, $m_1^\pi = 5.32$ GeV; the fit parameters are r_1, r_2, and $m_{\rm fit}$;

(ii) for $f^{K,\eta}_{+,T}$ and f^π_T (set 4):

$$f(q^2) = \frac{r_1}{1 - q^2/m_1^2} + \frac{r_2}{(1 - q^2/m_1^2)^2}, \tag{A2}$$

where m_1 is the mass of the 1^- meson in the corresponding channel cf. Table VI; the fit parameters are r_1 and r_2;

(iii) for f_0:

$$f_0(q^2) = \frac{r_2}{1 - q^2/m_{\rm fit}^2}, \tag{A3}$$

the fit parameters are r_2 and $m_{\rm fit}$.

The fit parameters are collected in the upper halves of Tables VIII and IX. Δ is a measure of the quality of the fit and defined as

TABLE IX. Fit parameters for K and η for Eq. (A2), for both the full form factors and the asymptotic ones, f^{as}, Eq. (A5), using the sets 2 and 4 in Table III. The form factor f_0 is fitted to the parametrization (A3). The mass parameters m_1 are given in Table VI. Δ is a measure of the quality of the fit and is defined in (A4).

	set 2, $m_b = 4.8$ GeV				set 4, $m_b = 4.6$ GeV			
	r_1	r_2	$m_{\rm fit}(m_1)$	Δ	r_1	r_2	$m_{\rm fit}(m_1)$	Δ
f_+^K	0.1616	0.1730	$(m_1^K)^2$	1.2	0.1903	0.1478	$(m_1^K)^2$	1.0
f_0^K	0	0.3302	37.46	1.0	0	0.3338	38.98	1.9
f_T^K	0.1614	0.1981	$(m_1^K)^2$	0.5	0.1851	0.1905	$(m_1^K)^2$	1.7
f_+^η	0.1220	0.1553	$(m_1^\eta)^2$	1.0	0.1380	0.1462	$(m_1^\eta)^2$	0.9
f_0^η	0	0.2734	31.03	0.5	0	0.2799	30.46	2.0
f_T^η	0.1108	0.1752	$(m_1^\eta)^2$	0.5	0.1160	0.1841	$(m_1^\eta)^2$	1.6
$f_+^{K,as}$	0.0541	0.2166	$(m_1^K)^2$	0.2	0.0991	0.2002	$(m_1^K)^2$	0.6
$f_0^{K,as}$	0	0.2719	30.33	0.7	0	0.2984	31.99	0.5
$f_T^{K,as}$	0.0244	0.2590	$(m_1^K)^2$	0.8	0.0660	0.2621	$(m_1^K)^2$	1.3
$f_+^{\eta,as}$	0.0802	0.1814	$(m_1^\eta)^2$	1.0	0.1201	0.1636	$(m_1^\eta)^2$	0.6
$f_0^{\eta,as}$	0	0.2604	28.80	0.5	0	0.2803	29.59	0.8
$f_T^{\eta,as}$	0.0570	0.2115	$(m_1^\eta)^2$	0.3	0.0914	0.2096	$(m_1^\eta)^2$	1.0

$$\Delta = 100 \max_t \left| \frac{f(t) - f^{\rm fit}(t)}{f(t)} \right|, \quad t \in \{0, \tfrac{1}{2}, \ldots, \tfrac{27}{2}, 14\} \text{ GeV}^2, \tag{A4}$$

i.e., it gives, in percent, the maximum deviation of the fitted form factors from the original LCSR result for $q^2 < 14$ GeV^2. From the Δ given in the table we conclude that the overall quality of the fits is very good and best for the pion and also that they work better for our preferred set 2 than for set 4.

2. Split form factors

As discussed in Sec. IV B, the values of the Gegenbauer moments $a_{1,2,4}$ are not very well-known. In Sec. IV D and Tables VIII and IX we have presented results only for our preferred choice of these parameters, i.e.,

$$a_1^K(1\text{ GeV}) = 0.17, \qquad a_2^{\pi,K,\eta}(1\text{ GeV}) = 0.115,$$
$$a_4^{\pi,K,\eta}(1\text{ GeV}) = -0.015, \qquad a_1^K(2.2\text{ GeV}) = 0.135,$$
$$a_2^{\pi,K,\eta}(2.2\text{ GeV}) = 0.080,$$
$$a_4^{\pi,K,\eta}(2.2\text{ GeV}) = -0.0089;$$

for set 4, the a_i are scaled up to $\mu_{\rm IR} = 2.6$ GeV. In order to allow the inclusion of future updates of these values, we split the form factors into contributions from different Gegenbauer moments. We define[14]

[13] Apart from f_T^π for set 4, which shows the same behavior as $f^{K,\eta}_{+,T}$ and hence is parametrized the same way, i.e., according to A 2.

[14] Note that this splitting is exact and valid for arbitrarily large a_i—there are no nonlinear terms in a_i.

$$f(q^2) = f^{as}(q^2) + a_1(\mu_{\rm IR})f^{a_1}(q^2) + a_2(\mu_{\rm IR})f^{a_2}(q^2) + a_4(\mu_{\rm IR})f^{a_4}(q^2), \tag{A5}$$

where f^{as} contains twist-2 contributions from the asymptotic DA and also all higher-twist contributions not proportional to $a_{1,2,4}$. The task is now to fit all functions f^{as,a_1,a_2,a_4}, in the interval $0 < q^2 < 14\,\text{GeV}^2$, to appropriate parametrizations.

For f^{as}, which gives the dominant contribution to all form factors, we use the same parametrization as for the full form factors. The results are collected in the lower halves of Tables VIII and IX. Again, the fits are very good and best for the pion and set 2.

The f^{a_i} turn out to be slowly varying functions of q^2, which can be fitted by a polynomial of 3rd degree:

$$f^{a_i}(q^2) = a + b(q^2) + c(q^2)^2 + d(q^2)^3. \tag{A6}$$

The measure of the quality of the fit has now to be defined in a slightly different way, as the f^{a_i} have zeros in the fit interval. We define the fit quality δ as

$$\delta = 100\frac{\sum_t |f(t) - f^{\rm fit}(t)|}{\sum_t |f(t)|}, \qquad t \in \{0, \tfrac{1}{2}, \ldots, \tfrac{27}{2}, 14\}\ \text{GeV}^2, \tag{A7}$$

i.e., as the average deviation of the fit from the true value, in percent. The fit parameters are given in Table V. As one can read off from the δ's, the fits are best for f^{a_1}, still good for f^{a_2}, and worst for f^{a_4}. The limited quality of the fits for f^{a_4} is due to a change of sign of its derivative at the upper end of the fit interval, which cannot be reliably reproduced by a polynomial of 3rd degree.

We would like to stress that none of the split form factor parametrizations must be used for q^2 larger than 14 GeV^2. For calculating the full form factors for arbitrary $a_{1,2,4}$, the following procedure should be followed:

(i) determine $a_{1,2,4}$ at the scale $\mu_{\rm IR}^2 = m_B^2 - m_b^2$; the scaling factors from $\mu = 1$ GeV up to 2.2 GeV (i.e., $m_b = 4.8$ GeV) are (0.793, 0.696, 0.590) for (a_1, a_2, a_4);
(ii) choose set 2 (preferred) or set 4;
(iii) calculate f^{as} from the appropriate formula (A1) and (A2) or (A3), using the fit parameters from Table VIII or IX;
(iv) calculate $f^{a_{1,2,4}}$ from (A6), using the fit parameters from Table V;
(v) calculate the total form factor from (A5);
(vi) extend the form factor to the full kinematical regime by fitting it to (A1) and (A2) or (A3).

APPENDIX B: DISTRIBUTION AMPLITUDES

In this appendix we collect explicit expressions for all the DAs that enter the form factors. These expressions are well-known and have been taken from Ref. [16].

The key point is that, to leading order in QCD, DAs can be expressed as a partial wave expansion in terms of contributions of increasing conformal spin, the so-called conformal expansion. The coefficients of different partial waves renormalize multiplicatively to LO in QCD, but mix at NLO, the reason being that the symmetry underlying the conformal expansion, the conformal symmetry of massless QCD, is anomalous and broken by radiative corrections.

The two-particle twist-2 amplitude (8) is expanded as

$$\phi(u, \mu) = \phi_{\rm as}(u)\sum_{n\geq 0} a_n(\mu)C_n^{3/2}(\zeta) \tag{B1}$$

with $\zeta \equiv 2u - 1$ and $a_0 = 1$ from normalization:

$$\int_0^1 du\phi(u, \mu) = 1.$$

The $C_n^{3/2}(\zeta)$ are Gegenbauer polynomials. The conformal spin of the term in $C_n^{3/2}$ is $j = n + 2$. For the π and η one has $a_{2n+1} = 0$ due to G-parity, but $a_1^K \sim (m_s - m_q)$ for the K [33], which is one source of SU(3) breaking for the form factors.

As only the first few Gegenbauer moments a_n are known numerically, we truncate the series at $n = 4$; the values of the conformal spins included are listed in Table X, whereas the numerical values of the a_i are discussed in Sec. IV. The truncation is justified as long as the perturbative kernels T with which the DAs are convoluted are slowly varying functions of u, so that the rapidly oscillating Gegenbauers suppress terms with high n. In our case the T are nonsingular for all u, including the end points $u = 0, 1$, so the truncation of the series is justified. The term labeled $\phi_{\rm as}$ in (B1) is the asymptotic DA which is reached for large scales $\mu \to \infty$; it is completely determined by perturbation theory and given by

$$\phi_{\rm as}(u) = 6u(1 - u);$$

it is the same for all mesons. The Gegenbauer moments a_n become relevant at moderate scales and depend on the hadron in question.

TABLE X. Overview of the contributions included in the calculations. For the K we also include conformal spin $j = 3$ for twist-2 which explicitly parametrizes SU(3) flavor breaking.

	tree					$O(\alpha_s)$				
twist	2	3		4		2	3		4	
x-particle	2	2	3	2	3	2	2	3	2	3
j_L	2	$\frac{3}{2}$	$\frac{7}{2}$	1	3	2	$\frac{3}{2}$	—	—	—
j_{NL}	4	$\frac{7}{2}$	$\frac{9}{2}$	3	5	4	$\frac{7}{2}$	—	—	—
j_{NNL}	6	$\frac{9}{2}$	—	5	—	6	—	—	—	—

TABLE XI. One-loop anomalous dimensions of hadronic parameters in DAs.

γ_{a_n}	γ_{η_3}	γ_{ω_3}	γ_{η_4}	γ_{ω_4}
$C_F(1 - \frac{2}{(n+1)(n+2)} + 4\sum_{m=2}^{n+1}\frac{1}{m})$	$\frac{16}{3}C_F + C_A$	$-\frac{7}{6}C_F + \frac{7}{3}C_A$	$\frac{8}{3}C_F$	$-\frac{8}{3}C_F + \frac{10}{3}C_A$

Let us now define the three-particle DAs. To twist-3 accuracy, there is only one:

$$\langle 0|\bar{u}(x)\sigma_{\mu\nu}\gamma_5 gG_{\alpha\beta}(vx)d(-x)|\pi^-(p)\rangle = i\frac{f_\pi m_\pi^2}{m_u + m_d}(p_\alpha p_\mu g_{\nu\beta} - p_\alpha p_\nu g_{\mu\beta} - p_\beta p_\mu g_{\nu\alpha} + p_\beta p_\nu g_{\alpha\mu})\mathcal{T}(v, p\cdot x) + \ldots, \tag{B2}$$

where the ellipses stand for Lorentz structures of twist-5 and higher and where we used the following short-hand notation for the integral defining the three-particle DA:

$$\mathcal{T}(v, p\cdot x) = \int \mathcal{D}\underline{\alpha} e^{-ip\cdot x(\alpha_u - \alpha_d + v\alpha_g)}\mathcal{T}(\alpha_d, \alpha_u, \alpha_g). \tag{B3}$$

Here $\underline{\alpha}$ is the set of three momentum fractions α_d (d quark), α_u (u quark), and α_g (gluon). The integration measure is defined as

$$\int \mathcal{D}\underline{\alpha} = \int_0^1 d\alpha_d d\alpha_u d\alpha_g \delta(1 - \alpha_u - \alpha_d - \alpha_g).$$

There are also four three-particle DAs of twist-4, defined as

$$\langle 0|\bar{u}(x)\gamma_\mu\gamma_5 gG_{\alpha\beta}(vx)d(-x)|\pi^-(p)\rangle = p_\mu(p_\alpha x_\beta - p_\beta x_\alpha)\frac{1}{p\cdot x}f_\pi m_\pi^2\mathcal{A}_\parallel(v, p\cdot x) + (p_\beta g_{\alpha\mu}^\perp - p_\alpha g_{\beta\mu}^\perp)f_\pi m_\pi^2\mathcal{A}_\perp(v, p\cdot x), \tag{B4}$$

$$\langle 0|\bar{u}(x)\gamma_\mu ig\tilde{G}_{\alpha\beta}(vx)d(-x)|\pi^-(p)\rangle = p_\mu(p_\alpha x_\beta - p_\beta x_\alpha)\frac{1}{p\cdot x}f_\pi m_\pi^2\mathcal{V}_\parallel(v, p\cdot x) + (p_\beta g_{\alpha\mu}^\perp - p_\alpha g_{\beta\mu}^\perp)f_\pi m_\pi^2\mathcal{V}_\perp(v, p\cdot x); \tag{B5}$$

$g_{\mu\nu}^\perp$ is defined as

$$g_{\mu\nu}^\perp = g_{\mu\nu} - \frac{1}{p\cdot x}(p_\mu x_\nu + p_\nu x_\mu).$$

To next-to-leading conformal spin ($j = 7/2, 9/2$), the twist-3 three-particle distribution amplitude $\mathcal{T}$ is given by[15]

$$\mathcal{T}(\alpha_u, \alpha_d, \alpha_g) = 360\eta_3\alpha_u\alpha_d\alpha_g^2\left\{1 + \omega_3\frac{1}{2}(7\alpha_g - 3)\right\}.$$

The two-particle twist-3 distribution amplitudes ϕ_p and ϕ_σ in Eqs. (9) and (10) depend on $\mathcal{T}$ through the equations of motions [16],[16] which implies that their coefficients are not independent from each other. The expansion up to NNL order ($j = 3/2, 7/2, 9/2$) reads[17]

$$\phi_p(u) = 1 + \left\{30\eta_3 - \frac{5}{2}\rho_\pi^2\right\}C_2^{1/2}(\zeta) + \left\{-3\eta_3\omega_3 - \frac{27}{20}\rho_\pi^2 - \frac{81}{10}\rho_\pi^2 a_2\right\}C_4^{1/2}(\zeta),$$

$$\phi_\sigma(u) = 6u(1-u)\left\{1 + \left\{5\eta_3 - \frac{1}{2}\eta_3\omega_3 - \frac{7}{20}\rho_\pi^2 - \frac{3}{5}\rho_\pi^2 a_2\right\}\right\}C_2^{3/2}(\zeta).$$

The two-particle twist-4 corrections g_π and $\mathbb{A}$ in Eq. (8) are given to NNL conformal spin ($j = 1, 3, 5$) by[18]

$$g_\pi(u) = 1 + \left\{1 + \frac{18}{7}a_2 + 60\eta_3 + \frac{20}{3}\eta_4\right\}C_2^{1/2}(\zeta) + \left\{-\frac{9}{28}a_2 - 6\eta_3\omega_3\right\}C_4^{1/2}(\zeta),$$

$$\mathbb{A}(u) = 6u\bar{u}\left\{\frac{16}{15} + \frac{24}{35}a_2 + 20\eta_3 + \frac{20}{9}\eta_4 + \left(-\frac{1}{15} + \frac{1}{16} - \frac{7}{27}\eta_3\omega_3 - \frac{10}{27}\eta_4\right)C_2^{3/2}(\xi) + \left(-\frac{11}{210}a_2 - \frac{4}{135}\eta_3\omega_3\right)C_4^{3/2}(\xi)\right\} + \left(-\frac{18}{5}a_2 + 21\eta_4\omega_4\right) \times\{2u^3(10 - 15u + 6u^2)\ln u + 2\bar{u}^3(10 - 15\bar{u} + 6\bar{u}^2)\ln\bar{u} + u\bar{u}(2 + 13u\bar{u})\}.$$

Finally the three-particle twist-4 DAs are to NL spin ($j = 3, 5$) given by

$$\mathcal{A}_\parallel[\underline{\alpha}] = 120\alpha_u\alpha_d\alpha_g(a_{10}(\alpha_d - \alpha_u)\},$$
$$\mathcal{V}_\parallel[\underline{\alpha}] = 120\alpha_u\alpha_d\alpha_g(v_{00} + v_{10}(3\alpha_g - 1)\},$$
$$\mathcal{A}_\perp(\underline{\alpha}) = 30\alpha_g^2[\alpha_u - \alpha_d][h_{00} + h_{01}\alpha_g + h_{10}(5\alpha_g - 3)/2\},$$
$$\mathcal{V}_\perp(\underline{\alpha}) = -30\alpha_g^2\{h_{00}\overline{\alpha}_g + h_{01}[\alpha_g\overline{\alpha}_g - 6\alpha_u\alpha_d] + h_{10}[\alpha_g\overline{\alpha}_g - 3/2(\alpha_u^2 + \alpha_d^2)]\},$$

where $\overline{\alpha} = 1 - \alpha$ and the a_{ij}, v_{ij}, and h_{ij} are related to hadronic matrix elements η_4, ω_4, and a_2 as

[15] In the literature the notation $f_{3\pi} = f_\pi\eta_3$ is also widely used.

[16] An explicit expression for ϕ_p in terms of $\mathcal{T}$ is given in Ref. [42], Eq. (16).

[17] At first glance it seems that ϕ_p is taken to a higher order in conformal expansion than ϕ_σ, but as discussed in the first reference of [16], ϕ_p and ϕ_σ are not pure spin projections, which means that the coefficients of a given Gegenbauer polynomial contain contributions from different partial waves.

[18] Note that, contrary to appearances, the contributions of g_π and $\mathbb{A}$ to (8) do not vanish for zero meson mass: η_4 implicitly contains a factor $1/m_\pi^2$ and survives in the limit $m_\pi^2 \to 0$.

$$a_{10} = \frac{21}{8}\eta_4\omega_4 - \frac{9}{20}a_2, \qquad v_{10} = \frac{21}{8}\eta_4\omega_4,$$
$$v_{00} = -\frac{1}{3}\eta_4, \qquad h_{01} = \frac{7}{4}\eta_4\omega_4 - \frac{3}{20}a_2,$$
$$h_{10} = \frac{7}{2}\eta_4\omega_4 + \frac{3}{20}a_2, \qquad v_{00} = -\frac{1}{3}\eta_4.$$

Taking everything together, we have seven hadronic parameters $\{c_i\} = \{a_1, a_2, a_4, \eta_3, \omega_3, \eta_4, \omega_4\}$ which parametrize all DAs to twist-4 and NLO in conformal spin. The c_i are scale dependent and are usually given at the scale 1 GeV. To LO in QCD, they do not mix under renormalization, so that the scaling up to $\mu_{\rm IR} = \sqrt{m_B^2 - m_b^2}$ is given by

$$c_i(\mu_{\rm IR}) = L^{\gamma_{c_i}/\beta_0} c_i(1\ \text{GeV}),$$

with $L = \alpha_s(\mu_{\rm IR})/\alpha_s(1\ \text{GeV})$, $\beta_0 = 11 - 2/3N_f$. The one-loop anomalous dimensions γ_{c_i} are given in Table XI. Note that the anomalous dimension increases with increasing conformal spin, $\gamma \sim \log j$, which implies that the truncation of the conformal expansion becomes better the higher the scale. The numerical values for all these parameters at the scale $\mu = 1$ GeV are collected in Table IV, taken from Ref. [16].

APPENDIX C: SPECTRAL DENSITIES FOR f_+

The total spectral density of Π_+ is obtained as sum of all the contributions listed below, i.e.,

$$\rho_{\Pi_+} = \rho_{\rm T2} + \rho_{\rm T3} + \rho_\sigma + \rho_p + \rho_{\rm T4}^{\rm 2p} + \rho_{\rm T4}^{\rm 3p}.$$

$\rho_{\rm T2}$ is the contribution from the twist-2 DA, $\rho_{\rm T3}$ from the twist-3 three-particle DA, $\rho_{\sigma(p)}$ from the twist-3 two-particle DA $\phi_{\sigma(p)}$, and $\rho_{\rm T4}^{\rm 2(3)p}$ from the two(three)-particle DAs of twist-4. There is also one constant term, $\mathrm{T4}_c$, which is due to twist-4 corrections that cannot be expressed via a dispersion relation, so that the total Borel-transformed Π_+ is given as

$$\hat{B}\Pi_+ = \int_{m_b^2}^\infty ds \rho_{\Pi_+}(s) e^{-s/M^2} + \mathrm{T4}_c.$$

We use $a_s = C_F \frac{\alpha_s}{4\pi}$

$$\begin{aligned}
\rho_{\rm T2} = {}& \frac{3f_\pi m_b}{(q^2-s)^7}(m_b^2-q^2)(m_b^2-s)[15a_4[42m_b^8 + q^8 + 10q^6 s + 20q^4 s^2 + 10q^2 s^3 + s^4 \\
& -84m_b^6(q^2+s) + 28m_b^4(2q^2+s)(q^2+2s) - 14m_b^2(q^2+s)(q^4+4q^2 s+s^2)] \\
& +(q^2-s)^2[6a_2[5m_b^4 + q^4 + 3q^2 s + s^2 - 5m_b^2(q^2+s)] + (q^2-s)[a_0(q^2-s) \\
& +3a_1(-2m_b^2+q^2+s)]]] + a_s\bigg\{\frac{3\mathbf{a_0} f_\pi m_b}{s(q^2-s)^3}\bigg[(m_b^2-s)[-2m_b^2 q^2 + 2q^4 + m_b^2(4+\pi^2)s \\
& -(1+\pi^2)q^2 s - 3s^2] + (m_b^2-q^2)\bigg[s(s-m_b^2)\log\bigg(1-\frac{q^2}{m_b^2}\bigg)^2 + s\log\bigg(\frac{s}{m_b^2}\bigg)\bigg[-2s + (m_b^2-s)\log\bigg(\frac{s}{m_b^2}\bigg)\bigg] \\
& +2(m_b^2-s)\bigg[2m_b^2 - 5s + s\log\bigg(\frac{s}{m_b^2}\bigg)\bigg[12m_b^4(q^2+s) + 14q^2 s(q^2+s) - 2m_b^2(4q^4+19q^2 s+7s^2) \\
& -3(m_b^2-q^2)(m_b^2-s)(2m_b^2-q^2-s)\log\bigg(\frac{s}{m_b^2}\bigg)\bigg] - 2(m_b^2-q^2)(s-m_b^2)(-2m_b^2+q^2+s) \\
& \times\bigg[6m_b^2 - 23s + 6s\log\bigg(\frac{s}{m_b^2}\bigg)\bigg]\log\bigg(\frac{s}{m_b^2}-1\bigg) + 6(m_b^2-q^2)s(s-m_b^2)(-2m_b^2+q^2+s)\log\bigg(\frac{s}{m_b^2}-1\bigg)^2 \\
& +6(m_b^2-q^2)(m_b^2-s)(2m_b^2-q^2-s)\log\bigg(1-\frac{q^2}{m_b^2}\bigg)\bigg[m_b^2 - s + s\log\bigg(\frac{s}{m_b^2}\bigg) - 2s\log\bigg(\frac{s}{m_b^2}-1\bigg)\bigg]\bigg] \\
& -18(m_b^2-q^2)(m_b^2-s)(2m_b^2-q^2-s)\bigg[\mathrm{Li}_2\bigg(\frac{q^2}{q^2-m_b^2}\bigg) + \mathrm{Li}_2\bigg(1-\frac{m_b^2}{s}\bigg) + 4\mathrm{Li}_2\bigg(1-\frac{s}{m_b^2}\bigg)\bigg]\bigg] \\
& + \frac{\mathbf{a_2} f_\pi m_b}{4s(q^2-s)^5}[(m_b^2-s)[-24(m_b^2-q^2)q^2(30m_b^4 - 15m_b^2 q^2 + q^4) + [5m_b^6(1183+72\pi^2) \\
& -20m_b^4(407+36\pi^2)q^2 + 12(5-6\pi^2)q^6 + 216m_b^2(11+2\pi^2)q^4]s - [5m_b^4(1525+72\pi^2) \\
& -16m_b^2(575+36\pi^2)q^2 + 36(73+6\pi^2)q^4]s^2 + [m_b^2(2083+72\pi^2) \\
& -8(260+9\pi^2)q^2]s^3 - 61s^4] + 12[25(m_b^2-q^2)(m_b^2-s)s[5m_b^4 + q^4 + 3q^2 s + s^2
\end{aligned}$$

$$- 5m_b^2(q^2 + s)]\log\left(\frac{\mu^2}{m_b^2}\right) - 6(m_b^2 - q^2)(m_b^2 - s)s[5m_b^4 + q^4 + 3q^2s + s^2$$
$$- 5m_b^2(q^2 + s)]\log\left(1 - \frac{q^2}{m_b^2}\right)^2 + s\log\left(\frac{s}{m_b^2}\right)\Big[-60m_b^6(q^2 + s)$$
$$+ 37q^2s(q^4 + 3q^2s + s^2) + 30m_b^4(3q^4 + 8q^2s + 3s^2) - m_b^2(25q^6 + 237q^4s$$
$$+ 261q^2s^2 + 37s^3) + 6(m_b^2 - q^2)(m_b^2 - s)[5m_b^4 + q^4 + 3q^2s + s^2$$
$$- 5m_b^2(q^2 + s)]\log\left(\frac{s}{m_b^2}\right)\Big] + 2(m_b^2 - q^2)(m_b^2 - s)[5m_b^4 + q^4 + 3q^2s + s^2$$
$$- 5m_b^2(q^2 + s)]\Big[12m_b^2 - 55s + 12s\log\left(\frac{s}{m_b^2}\right)\Big]\log\left(\frac{s}{m_b^2} - 1\right)$$
$$+ 12s(m_b^2 - q^2)(s - m_b^2)[5m_b^4 + q^4 + 3q^2s + s^2 - 5m_b^2(q^2 + s)]\log\left(\frac{s}{m_b^2} - 1\right)^2$$
$$- 12(m_b^2 - q^2)(m_b^2 - s)[5m_b^4 + q^4 + 3q^2s + s^2 - 5m_b^2(q^2 + s)]\log\left(1 - \frac{q^2}{m_b^2}\right)$$
$$\times\Big[m_b^2 - s + s\log\left(\frac{s}{m_b^2}\right) - 2s\log\left(\frac{s}{m_b^2} - 1\right)\Big]] + 144(m_b^2 - q^2)(m_b^2 - s)[5m_b^4 + q^4$$
$$+ 3q^2s + s^2 - 5m_b^2(q^2 + s)]\Big[\mathrm{Li}_2\left(\frac{q^2}{q^2 - m_b^2}\right) + \mathrm{Li}_2\left(1 - \frac{m_b^2}{s}\right) + 4\mathrm{Li}_2\left(1 - \frac{s}{m_b^2}\right)\Big]]$$
$$+ \frac{\mathbf{a_4} f_\pi m_b}{10s(q^2 - s)^7}[-[(m_b^2 - s)[30(m_b^2 - q^2)q^2(1260m_b^8 - 1890m_b^6q^2 - 105m_b^2q^6 + 2q^8$$
$$+ 840m_b^4q^4) - [21m_b^{10}(23207 + 900\pi^2) - 63m_b^8(18827 + 900\pi^2)q^2 - 700m_b^4(439 + 45\pi^2)q^6$$
$$+ 150m_b^2(176 + 45\pi^2)q^8 + 30(19 - 15\pi^2)q^{10} + 175m_b^6(5603 + 360\pi^2)q^4]s$$
$$+ 84[m_b^8(13051 + 450\pi^2) - 112m_b^6(22157 + 900\pi^2)q^2 - 800m_b^2(616 + 45\pi^2)q^6$$
$$+ 150(283 + 30\pi^2)q^8 + 525m_b^4(3523 + 180\pi^2)q^4]s^2[-7m_b^6(119363 + 3600\pi^2)$$
$$+ 756m_b^4(2131 + 75\pi^2)q^2 + 200(848 + 45\pi^2)q^6 - 10125m_b^2(89 + 4\pi^2)q^4]s^3$$
$$+ [7m_b^4(34967 + 900\pi^2) - 6m_b^2(57989 + 1800\pi^2)q^2 + 125(1075 + 36\pi^2)q^4]s^4$$
$$+ [-2m_b^2(10553 + 225\pi^2) + (21461 + 450\pi^2)q^2]s^5 + 181s^6]]$$
$$+ 30\Big[91(m_b^2 - q^2)(m_b^2 - s)s[42m_b^8 + q^8 + 10q^6s + 20q^4s^2 + 10q^2s^3 + s^4 - 84m_b^6(q^2 + s)$$
$$+ 28m_b^4(2q^2 + s)(q^2 + 2s) - 14m_b^2(q^2 + s)(q^4 + 4q^2s + s^2)]\log\left(\frac{\mu^2}{m_b^2}\right)$$
$$- 15(m_b^2 - q^2)(m_b^2 - s)s(42m_b^8 + q^8 + 10q^6s + 20q^4s^2 + 10q^2s^3 + s^4 - 84m_b^6)(q^2 + s)$$
$$+ 28m_b^4(2q^2 + s)(q^2 + 2s) - 14m_b^2(q^2 + s)(q^4 + 4q^2s + s^2)\Big]\log\left(1 - \frac{q^2}{m_b^2}\right)^2$$
$$+ s\log\left(\frac{s}{m_b^2}\right)\Big[-1260m_b^{10}(q^2 + s) + 630m_b^8(5q^4 + 12q^2s + 5s^2) - 210m_b^6(q^2 + s)(13q^4$$
$$+ 48q^2s + 13s^2) + 121q^2s(q^8 + 10q^6s + 20q^4s^2 + 10q^2s^3 + s^4) + 105m_b^4(9q^8 + 82q^6s$$
$$+ 160q^4s^2 + 82q^2s^3 + 9s^4) - m_b^2(91q^{10} + 2305q^8s + 9400q^6s^2 + 9700q^4s^3$$
$$+ 2575q^2s^4 + 121s^5) + 15(m_b^2 - q^2)(m_b^2 - s)[42m_b^8 + q^8 + 10q^6s + 20q^4s^2$$
$$+ 10q^2s^3 + s^4 - 84m_b^6(q^2 + s) + 28m_b^4(2q^2 + s)(q^2 + 2s) - 14m_b^2(q^2 + s)(q^4$$
$$+ 4q^2s + s^2)]\log\left(\frac{s}{m_b^2}\right)\Big] + 4(m_b^2 - q^2)(m_b^2 - s)[42m_b^8 + q^8 + 10q^6s$$

$$+20q^4s^2 + 10q^2s^3 + s^4 - 84m_b^6(q^2+s) + 28m_b^4(2q^2+s)(q^2+2s)$$
$$-14m_b^2(q^2+s)(q^4+4q^2s+s^2)]\left[15m_b^2 - 83s + 15s\log\left(\frac{s}{m_b^2}\right)\right]\log\left(\frac{s}{m_b^2}-1\right)$$
$$+30(m_b^2-q^2)s(s-m_b^2)[42m_b^8 + q^8 + 10q^6s + 20q^4s^2 + 10q^2s^3 + s^4 - 84m_b^6(q^2+s)$$
$$+28m_b^4(2q^2+s)(q^2+2s) - 14m_b^2(q^2+s)(q^4+4q^2s+s^2)]\log\left(\frac{s}{m_b^2}-1\right)^2$$
$$-30(m_b^2-q^2)(m_b^2-s)[42m_b^8 + q^8 + 10q^6s + 20q^4s^2 + 10q^2s^3 + s^4 - 84m_b^6(q^2+s)$$
$$+28m_b^4(2q^2+s)(q^2+2s) - 14m_b^2(q^2+s)(q^4+4q^2s+s^2)]\log\left(1-\frac{q^2}{m_b^2}\right)\left[m_b^2 - s\right.$$
$$\left.+s\log\left(\frac{s}{m_b^2}\right) - 2s\log\left(\frac{s}{m_b^2}-1\right)\right]] + 900s(m_b^2-q^2)(m_b^2-s)[42m_b^8 + q^8 + 10q^6s$$
$$+20q^4s^2 + 10q^2s^3 + s^4 - 84m_b^6(q^2+s) + 28m_b^4(2q^2+s)(q^2+2s)$$
$$-14m_b^2(q^2+s)(q^4+4q^2s+s^2)]\left[\mathrm{Li}_2\left(\frac{q^2}{q^2-m_b^2}\right) + \mathrm{Li}_2\left(1-\frac{m_b^2}{s}\right) + 4\mathrm{Li}_2\left(1-\frac{s}{m_b^2}\right)\right]\Bigg\}$$

$$\rho_{T3} = \frac{-15\eta_3\mu_\pi^2}{(q^2-s)^6}(m_b^2-q^2)^2(m_b^2-s)[2(q^2-s)(-5m_b^2+2q^2+3s) + (7m_b^4 - 6m_b^2q^2 + q^4 - 8m_b^2s + 4q^2s + 2s^2)\omega_3]$$

$$\rho_p = \frac{a_0\mu_\pi^2(3m_b^2s - 3q^2s)}{6(q^2-s)^2s} + \frac{5\eta_3\mu_\pi^2}{(q^2-s)^4s}(18m_b^6s - 36m_b^4q^2s - 3q^6s + 21m_b^2q^4s - 18m_b^4s^2$$
$$+30m_b^2q^2s^2 - 12q^4s^2 + 3m_b^2s^3 - 3q^2s^3) + \alpha_s\Bigg\{\frac{\mathbf{a_0}\mu_\pi^2}{6(q^2-s)^2s}\Bigg((q^2+s)(s-3m_b^2)$$
$$-3(m_b^2-4q^2)s\log\left(\frac{q^2}{m_b^2}\right)^2 - 18s(3m_b^2-3q^2+s)\log\left(1-\frac{q^2}{m_b^2}\right)^2(m_b^2-4q^2)s\log\left(\frac{q^2}{m_b^2}\right)$$
$$\times\left(\log\left(1-\frac{q^2}{m_b^2}\right) - \log\left(\frac{s-q^2}{m_b^2}\right)\right) + 6\log\left(1-\frac{q^2}{m_b^2}\right)\Bigg(m_b^2q^2 + 3m_b^2s - q^2s$$
$$+s\Bigg((2m_b^2-3q^2)\log\left(\frac{\mu^2}{m_b^2}\right) + q^2\log\left(\frac{s}{m_b^2}\right)(m_b^2+q^2+s)\log\left(\frac{s-q^2}{m_b^2}\right)$$
$$-(m_b^2-2q^2)\log\left(\frac{s}{m_b^2}-1\right)\Bigg)\Bigg) + 3\Bigg(m_b^2s\log\left(\frac{s}{m_b^2}\right)^2 - \log\left(\frac{s-q^2}{m_b^2}\right)^2s(5q^2+s)$$
$$+\log\left(\frac{s}{m_b^2}\right)\left(2m_b^2q^2 + m_b^2s - 3q^2s - 4q^2s\log\left(\frac{s}{m_b^2}-1\right)\right) + 2\log\left(\frac{s-q^2}{m_b^2}\right)\Bigg(2q^2s - m_b^2(q^2+s)$$
$$-s(2m_b^2-3q^2+s)\log\left(\frac{\mu^2}{m_b^2}\right) + s(3m_b^2-2q^2+2s)\log\left(\frac{s}{m_b^2}-1\right)\Bigg)$$
$$+2\log\left(\frac{s}{m_b^2}-1\right)\Bigg(2q^2s - m_b^2(q^2+4s) + s\left(s\log\left(\frac{\mu^2}{m_b^2}\right) - (m_b^2+2s)\log\left(\frac{s}{m_b^2}-1\right)\right)\Bigg)\Bigg)\Bigg)$$

$$+6s\left(m_b^2\mathrm{Li}_2\left(\frac{q^2}{q^2-m_b^2}\right)+(2m_b^2-3q^2+s)\mathrm{Li}_2\left(1-\frac{q^2}{m_b^2}\right)\right.$$
$$+m_b^2\mathrm{Li}_2\left(1-\frac{m_b^2}{s}\right)-(m_b^2+q^2+s)\mathrm{Li}_2\left(1-\frac{q^2}{s}\right)$$
$$-(5q^2+s)\mathrm{Li}_2\left(\frac{m_b^2-s}{m_b^2-q^2}\right)-(m_b^2+q^2+s)\mathrm{Li}_2\left(\frac{m_b^2-s}{q^2-s}\right)$$
$$-(m_b^2+q^2+s)\mathrm{Li}_2\left(\frac{(q^2-m_b^2)s}{m_b^2(q^2-s)}\right)+(2m_b^2-3q^2+s)\mathrm{Li}_2\left(\frac{m_b^2-q^2}{s-q^2}\right)$$
$$\left.\left.+2(m_b^2-q^2)\mathrm{Li}_2\left(1-\frac{s}{m_b^2}\right)+(m_b^2-4q^2)\mathrm{Li}_2\left(1-\frac{s}{q^2}\right)\right)\right)6(q^2-s)^2s$$
$$+\frac{5\eta_3\mu_\pi^2}{(q^2-s)^4s}\left(-3m_b^2(q^2-12m_b^2)q^4-6m_b^6(\pi^2-47)s\right.$$
$$-18m_b^4(24+\pi^2)q^2s+(3+2\pi^2)q^6s+3m_b^2(8\pi^2-17)q^4s$$
$$+6m_b^4(\pi^2-60)s^2+3m_b^2(205+6\pi^2)q^2s^2-(3+26\pi^2)q^4s^2$$
$$+69m_b^2s^3-(147+2\pi^2)q^2s^3+(-9+2\pi^2)s^4$$
$$+3(m_b^2-4q^2)(q^2-s)^2s\log\left(\frac{q^2}{m_b^2}\right)^2+6(m_b^2-4q^2)(q^2-s)^2s\log\left(\frac{q^2}{m_b^2}\right)$$
$$\times\left(\log\left(1-\frac{q^2}{m_b^2}\right)-\log\left(\frac{s-q^2}{m_b^2}\right)\right)+6s\log\left(\frac{\mu^2}{m_b^2}\right)\left(15m_b^6-15m_b^4(2q^2+s)\right.$$
$$-3q^2s(q^2+4s)+m_b^2(9q^4+30q^2s+6s^2)+(6m_b^6-6m_b^4s$$
$$-3q^2(q^4-4q^2s+s^2)+m_b^2(-4q^4-4q^2s+2s^2))$$
$$\times\log\left(1-\frac{q^2}{m_b^2}\right)-(q^2-s)^2(2m_b^2-3q^2+s)\log\left(\frac{s-q^2}{m_b^2}\right)$$
$$+(-6m_b^6+6m_b^2q^4+6m_b^4s+s(-5q^4-2q^2s+s^2))$$
$$\left.\times\log\left(\frac{s}{m_b^2}-1\right)\right)+3\left(-\left(s(6m_b^6-(q^2-s)^2(3q^2-s)\right.\right.$$
$$\left.-6m_b^4(q^2+s)+3m_b^2(q^4+s^2))-\log\left(1-\frac{q^2}{m_b^2}\right)^2\right)$$
$$+m_b^2s(6m_b^4+q^4+4q^2s+s^26m_b^2(q^2+s))\log\left(\frac{s}{m_b^2}\right)^2$$
$$-(q^2-s)^2\log\left(\frac{s-q^2}{m_b^2}\right)(2(-2q^2s+m_b^2(q^2+s))$$
$$+s(5q^2+s)\log\left(\frac{s-q^2}{m_b^2}\right)\bigg)2\bigg(6m_b^6(2q^2+9s)$$
$$-6m_b^4(2q^4+18q^2s+9s^2)-2q^2s(q^4+7q^2s+13s^2)$$
$$+m_b^2(q^6+44q^4s+89q^2s^2+16s^3)(-3m_b^2+2q^2$$
$$-2s)(q^2-s)^2s\log\left(\frac{s-q^2}{m_b^2}\right)\bigg)\log\left(\frac{s}{m_b^2}-1\right)-2s(-6m_b^6-6m_b^4(q^2-s)$$
$$+2s(-5q^4-2q^2s+s^2)m_b^2(13q^4+4q^2s+s^2))\log\left(\frac{s}{m_b^2}-1\right)^2$$
$$+\log\left(\frac{s}{m_b^2}\right)\left(-12m_b^4s^2-3q^2s(q^2+3s)^2+m_b^2(2q^6+21q^4s+12q^2s^2+13s^3)\right)$$

$$
\begin{aligned}
&-4q^2s(6m_b^4+q^4+4q^2s+s^2-6m_b^2(q^2+s))\log\left(\frac{s}{m_b^2}-1\right)\Big)\\
&+2\log\left(1-\frac{q^2}{m_b^2}\right)\Big(6m_b^6(q^2+2s)-q^2s(q^4-8q^2s+s^2)\\
&-6m_b^4(q^4+2q^2s+2s^2)+m_b^2(q^6+q^4s+q^2s^2+3s^3)\\
&+s(q^2(6m_b^4+q^4+4q^2s+s^2-6m_b^2(q^2+s))\log\left(\frac{s}{m_b^2}\right)\\
&+(q^2-s)^2(m_b^2+q^2+s)\log\left(\frac{s-q^2}{m_b^2}\right)+(-12m_b^4q^2+m_b^2(11q^4\\
&+14q^2s-s^2)+2q^2(q^4-8q^2s+s^2))\log\left(\frac{s}{m_b^2}-1\right)\Big)\Big)\Big)\\
&+6s\Big(m_b^2(6m_b^4+q^4+4q^2s+s^2-6m_b^2(q^2+s))\mathrm{Li}_2\left(\frac{q^2}{q^2-m_b^2}\right)\\
&+(q^2-s)^2(2m_b^2-3q^2+s)\mathrm{Li}_2\left(1-\frac{q^2}{m_b^2}\right)+m_b^2(6m_b^4+q^4+4q^2s\\
&+s^2-6m_b^2(q^2+s))\mathrm{Li}_2\left(1-\frac{m_b^2}{s}\right)(q^2-s)^2(m_b^2+q^2+s)\mathrm{Li}_2\left(1-\frac{q^2}{s}\right)\\
&-(q^2-s)^2(5q^2+s)\mathrm{Li}_2\left(\frac{m_b^2-s}{m_b^2-q^2}\right)-(q^2-s)^2(m_b^2+q^2+s)\mathrm{Li}_2\left(\frac{m_b^2-s}{q^2-s}\right)\\
&-(q^2-s)^2(m_b^2+q^2+s)\mathrm{Li}_2\left(\frac{(q^2-m_b^2)s}{m_b^2(q^2-s)}\right)+(q^2-s)^2(2m_b^2-3q^2\\
&+s)\mathrm{Li}_2\left(\frac{m_b^2-q^2}{s-q^2}\right)+2(m_b^2-q^2)(6m_b^4+q^4+4q^2s+s^2\\
&-6m_b^2(q^2+s))\mathrm{Li}_2\left(1-\frac{s}{m_b^2}\right)+(m_b^2-4q^2)(q^2-s)^2\mathrm{Li}_2\left(1-\frac{s}{q^2}\right)\Big)\Big]\Big\}
\end{aligned}
$$

$$
\begin{aligned}
\rho_\sigma=&\frac{\mu_\pi^2}{2(q^2-s)^5}(a_0(q^2-s)^2(-(m_b^2(3q^2+s))+q^2(q^2+3s))-30\eta_3(10m_b^8\\
&+10m_b^6(q^2-s)\vec{W}-30m_b^4q^2(q^2+s)+m_b^2(13q^6+45q^4s+21q^2s^2+s^3)\\
&-q^2(q^6+11q^4s+15q^2s^2+3s^3)))+\alpha_s\Big\{\frac{\mathbf{a_0}\mu_\pi^2}{6(q^2-s)^3s}\Big(3m_b^2q^4\\
&+q^2(-4m_b^2(-9+\pi^2)+(-3+2\pi^2)q^2)s+(m_b^2(21-4\pi^2)\\
&+4(-15+\pi^2)q^2)s^2+(3+2\pi^2)s^3+6s(-4q^2s+m_b^2(3q^2\\
&+s))\log\left(1-\frac{q^2}{m_b^2}\right)^2+6s\log\left(\frac{\mu^2}{m_b^2}\right)\Big(3(-2q^2s+m_b^2(q^2+s))\\
&+(q^2-s)\Big(-\Big((m_b^2+q^2)\log\left(1-\frac{q^2}{m_b^2}\right)\Big)\Big)-(m_b^2+q^2\\
&+s)\log\left(\frac{m_b^2-s}{q^2-s}\right)-(m_b^2-4q^2)\log\left(\frac{m_b^2-q^2}{s-q^2}\right)+(m_b^2\\
&+q^2)\log\left(\frac{s}{m_b^2}-1\right)\Big)\Big)\Big)+3\Big(-2(q^2-s)s(m_b^2+q^2+s)\log\left(\frac{s}{m_b^2}\right)^2
\end{aligned}
$$

$$
\begin{aligned}
&+2(q^2-s)\log\left(\frac{m_b^2-s}{q^2-s}\right)\left(-(m_b^2(q^2+2s))+s(m_b^2+q^2+s)\log\left(\frac{s-q^2}{m_b^2}\right)\right)\\
&+(q^2-s)s\left((m_b^2+q^2+s)\log\left(\frac{m_b^2-q^2}{s-q^2}\right)^2-(m_b^2+q^2+s)\log\left(\frac{(m_b^2-q^2)s}{m_b^2(s-q^2)}\right)^2\right.\\
&-2(m_b^2+q^2+s)\log\left(\frac{(m_b^2-q^2)s}{m_b^2(s-q^2)}\right)\log\left(\frac{s-q^2}{m_b^2}\right)+2(2m_b^2-3q^2+s)\log\left(\frac{s-q^2}{m_b^2}\right)^2\\
&\left.+2\log\left(\frac{m_b^2-q^2}{s-q^2}\right)\left(-3m_b^2+6q^2+(2m_b^2-3q^2+s)\log\left(\frac{s-q^2}{m_b^2}\right)\right)\right)-2\left(4m_b^4(q^2+s)\right.\\
&+2q^2s(q^2+3s)-2m_b^2q^2(q^2+7s)+(q^2-s)s(5m_b^2-5q^2+3s)\log\left(\frac{s-q^2}{m_b^2}\right)\Big)\log\left(\frac{s}{m_b^2}-1\right)\\
&+2s(-2s(q^2+s)+m_b^2(3q^2+s))\log\left(\frac{s}{m_b^2}-1\right)^2+\log\left(\frac{s}{m_b^2}\right)\left(q^2s(3q^2+s)\right.\\
&-m_b^2(q^2-s)(2q^2+5s)-2(q^2-s)s(m_b^2+q^2+s)\left(\log\left(\frac{m_b^2-q^2}{s-q^2}\right)-\log\left(\frac{(m_b^2-q^2)s}{m_b^2(s-q^2)}\right)\right.\\
&\left.\left.\left.-\log\left(\frac{s-q^2}{m_b^2}\right)\right)+2s(-5m_b^2q^2+q^4-3m_b^2s+6q^2s+s^2)\log\left(\frac{s}{m_b^2}-1\right)\right)\right)\\
&+6\log\left(1-\frac{q^2}{m_b^2}\right)\left(-(q^2(q^2-7s)s)+2m_b^4(q^2+2s)-m_b^2(q^4+9q^2s+2s^2)\right.\\
&+s\left((4q^2s-m_b^2(3q^2+s))\log\left(\frac{q^2}{m_b^2}\right)+(2m_b^2(q^2+s)-q^2(q^2+3s))\log\left(\frac{s}{m_b^2}\right)\right.\\
&+(q^2-s)\left(-\left((m_b^2+q^2+s)\left(\log\left(\frac{m_b^2-q^2}{s-q^2}\right)-\log\left(\frac{(m_b^2-q^2)s}{m_b^2(s-q^2)}\right)\right)\right)\right.\\
&\left.\left.\left.-(m_b^2-4q^2)\log\left(\frac{s-q^2}{m_b^2}\right)\right)-2(q^2(3q^2-7s)+m_b^2(q^2+3s))\log\left(\frac{s}{m_b^2}-1\right)\right)\right)\\
&+6s((4q^2s-m_b^2(3q^2+s))\mathrm{Li}_2\left(1-\frac{q^2}{m_b^2}\right)-(m_b^2-4q^2)(q^2-s)\left(2\mathrm{Li}_2\left(\frac{m_b^2-s}{m_b^2-q^2}\right)\right.\\
&\left.\left.\left.+\mathrm{Li}_2\left(\frac{m_b^2-s}{q^2-s}\right)-\mathrm{Li}_2\left(\frac{q^2(m_b^2-s)}{m_b^2(q^2-s)}\right)\right)-(3m_b^2(3q^2+s)-(q^2+s)(5q^2+s))\mathrm{Li}_2\left(1-\frac{s}{m_b^2}\right)\right)\right)\\
&+\frac{5\eta_3\mu_\pi^2}{6(q^2-s)^5s}(18m_b^2q^4(40m_b^4-40m_b^2q^2+q^4)+(5m_b^8(-359+24\pi^2)\\
&-30m_b^6(127+16\pi^2)q^2+30m_b^4(129+20\pi^2)q^4+24m_b^2(40-11\pi^2)q^6\\
&+6(-3+2\pi^2)q^8)s+2(5m_b^6(295-36\pi^2)+30m_b^4(129+16\pi^2)q^2-6m_b^2(609\\
&+68\pi^2)q^4+6(-27+20\pi^2)q^6)s^2+6(5m_b^4(-25+8\pi^2)-19m_b^2(39+4\pi^2)q^2\\
&+9(55+4\pi^2)q^4)s^3-4(m_b^2(71+6\pi^2)-66q^2)s^4+(-37+12\pi^2)s^5+36s(10m_b^8\\
&-10m_b^6s-10m_b^4q^2(q^2+2s)-4q^2s(q^4+3q^2s+s^2)+m_b^2(3q^6+25q^4s+21q^2s^2\\
&+s^3))\log\left(1-\frac{q^2}{m_b^2}\right)^2+12s\log\left(\frac{\mu^2}{m_b^2}\right)\left(-(m_b^2(5m_b^2-2q^2)(5m_b^4+20m_b^2q^2-28q^4))\right.\\
&+(40m_b^6+135m_b^4q^2-249m_b^2q^4+47q^6)s-3(5m_b^4+18m_b^2q^2-32q^4)s^2\\
&+9(m_b^2-2q^2)s^3-3(10m_b^8-20m_b^6(q^2+s)+10m_b^4(q^2+s)(2q^2+s)+q^2(q^6\\
&+7q^4s+3q^2s^2-s^3)-m_b^2(9q^6+23q^4s+7q^2s^2+s^3))\log\left(1-\frac{q^2}{m_b^2}\right)
\end{aligned}
$$

$$
\begin{aligned}
&+3(q^2-s)^3\bigg(-\bigg((m_b^2+q^2+s)\log\bigg(\frac{m_b^2-s}{q^2-s}\bigg)\bigg)-(m_b^2-4q^2)\log\bigg(\frac{m_b^2-q^2}{s-q^2}\bigg)\bigg)+3\bigg(10m_b^8-20m_b^6(q^2+s)\\
&+10m_b^4(q^2+s)(2q^2+s)+q^2(q^6+7q^4s+3q^2s^2-s^3)-m_b^2(9q^6+23q^4s+7q^2s^2+s^3)\big)\log\bigg(\frac{s}{m_b^2}-1\bigg)\bigg)\\
&+36\log\bigg(1-\frac{q^2}{m_b^2}\bigg)\bigg(20m_b^8q^2-10m_b^6q^2(3q^2+5s)+2m_b^4(q^2+2s)(6q^4+13q^2s+s^2)-q^2s(q^6+q^4s-15q^2s^2\\
&-7s^3)-m_b^2(q^8+7q^6s+35q^4s^2+35q^2s^3+2s^4)+s\bigg((-10m_b^8+10m_b^6s+10m_b^4q^2(q^2+2s)+4q^2s(q^4+3q^2s\\
&+s^2)-m_b^2(3q^6+25q^4s+21q^2s^2+s^3))\log\bigg(\frac{q^2}{m_b^2}\bigg)+(10m_b^6(2q^2+s)-10m_b^4(3q^4+5q^2s+s^2)+2m_b^2(6q^6\\
&+24q^4s+14q^2s^2+s^3)-q^2(q^6+11q^4s+15q^2s^2+3s^3))\log\bigg(\frac{s}{m_b^2}\bigg)+(q^2-s)^3\bigg(-\bigg((m_b^2+q^2+s)\bigg(\log\bigg(\frac{m_b^2-q^2}{s-q^2}\bigg)\\
&-\log\bigg(\frac{(m_b^2-q^2)s}{m_b^2(s-q^2)}\bigg)\bigg)\bigg)-(m_b^2-4q^2)\log\bigg(\frac{s-q^2}{m_b^2}\bigg)\bigg)-2(10m_b^6(2q^2+s)-10m_b^4(3q^4+5q^2s+s^2)+q^2(3q^6-23q^4s\\
&-3q^2s^2-7s^3)+m_b^2(11q^6+51q^4s+25q^2s^2+3s^3))\log\bigg(\frac{s}{m_b^2}-1\bigg)\bigg)\bigg)+6\bigg(-6(q^2-s)^3s(m_b^2+q^2+s)\log\bigg(\frac{s}{m_b^2}\bigg)^2\\
&+6(q^2-s)^3\log\bigg(\frac{m_b^2-s}{q^2-s}\bigg)\bigg(-(m_b^2(q^2+2s))+s(m_b^2+q^2+s)\log\bigg(\frac{s-q^2}{m_b^2}\bigg)\bigg)+3(q^2-s)^3s\bigg((m_b^2+q^2\\
&+s)\log\bigg(\frac{m_b^2-q^2}{s-q^2}\bigg)^2-(m_b^2+q^2+s)\log\bigg(\frac{(m_b^2-q^2)s}{m_b^2(s-q^2)}\bigg)^2-2(m_b^2+q^2+s)\log\bigg(\frac{(m_b^2-q^2)s}{m_b^2(s-q^2)}\bigg)\log\bigg(\frac{s-q^2}{m_b^2}\bigg)\\
&+2(2m_b^2-3q^2+s)\log\bigg(\frac{s-q^2}{m_b^2}\bigg)^2+2\log\bigg(\frac{m_b^2-q^2}{s-q^2}\bigg)\bigg(-3m_b^2+6q^2+(2m_b^2-3q^2+s)\log\bigg(\frac{s-q^2}{m_b^2}\bigg)\bigg)\bigg)\\
&+2\bigg(m_b^8(-120q^2+170s)+20m_b^6(9q^4+24q^2s-10s^2)-6m_b^4(12q^6+148q^4s+123q^2s^2-3s^3)\\
&-2q^2s(3q^6+98q^4s+195q^2s^2+9s^3)+2m_b^2q^2(3q^6+140q^4s+531q^2s^2+216s^3)+3s(s\\
&-q^2)^3(5m_b^2-5q^2+3s)\log\bigg(\frac{s-q^2}{m_b^2}\bigg)\bigg)\log\bigg(\frac{s}{m_b^2}-1\bigg)-6s(10m_b^8-10m_b^6(4q^2+3s)+2s(q^2+s)(11q^4\\
&-2q^2s+s^2)+10m_b^4(5q^4+8q^2s+2s^2)-m_b^2(23q^6+65q^4s+41q^2s^2+s^3))\log\bigg(\frac{s}{m_b^2}-1\bigg)^2\\
&+\log\bigg(\frac{s}{m_b^2}\bigg)\bigg(-6m_b^2q^8+q^4(120m_b^4-157m_b^2q^2+9q^4)s+(60m_b^6+60m_b^4q^2-243m_b^2q^4+205q^6)s^2-3(10m_b^4\\
&+43m_b^2q^2-121q^4)s^3+3(5m_b^2+q^2)s^4-6(q^2-s)^3s(m_b^2+q^2+s)\bigg(\log\bigg(\frac{m_b^2-q^2}{s-q^2}\bigg)-\log\bigg(\frac{(m_b^2-q^2)s}{m_b^2(s-q^2)}\bigg)\\
&-\log\bigg(\frac{s-q^2}{m_b^2}\bigg)\bigg)+6s(q^8+24q^6s+30q^4s^2+4q^2s^3+s^4-20m_b^6(2q^2+s)+20m_b^4(3q^4+5q^2s+s^2)\\
&-m_b^2(25q^6+93q^4s+59q^2s^2+3s^3))\log\bigg(\frac{s}{m_b^2}-1\bigg)\bigg)\bigg)+36s((-10m_b^8+10m_b^6s+10m_b^4q^2(q^2+2s)\\
&+4q^2s(q^4+3q^2s+s^2)-m_b^2(3q^6+25q^4s+21q^2s^2+s^3))\mathrm{Li}_2\bigg(1-\frac{q^2}{m_b^2}\bigg)-(m_b^2-4q^2)(q^2-s)^3\bigg(2\mathrm{Li}_2\bigg(\frac{m_b^2-s}{m_b^2-q^2}\bigg)\\
&+\mathrm{Li}_2\bigg(\frac{m_b^2-s}{q^2-s}\bigg)-\mathrm{Li}_2\bigg(\frac{q^2(m_b^2-s)}{m_b^2(q^2-s)}\bigg)\bigg)-(10m_b^8-5q^8-16q^6s-54q^4s^2-4q^2s^3-s^4+10m_b^6(4q^2+s)\\
&-10m_b^4(7q^4+12q^2s+2s^2)+m_b^2(29q^6+115q^4s+83q^2s^2+3s^3))\mathrm{Li}_2\bigg(1-\frac{s}{m_b^2}\bigg)\bigg)\bigg\}
\end{aligned}
$$

$$\rho^{2p}_{\mathrm{T4}} = \frac{f_\pi m_b \mu_\pi^2}{120(q^2-s)^7}\Big[27a_2[2880m_b^{10} - 25m_b^8(215q^2+229s) + 20m_b^6(149q^4+447q^2s+184s^2) - 10m_b^4(38q^6 + 352q^4s + 427q^2s^2 + 83s^3) + 5q^2(q^8+17q^6s+42q^4s^2+22q^2s^3+2s^4) + m_b^2(-76q^8+84q^6s+584q^4s^2 + 584q^2s^3+24s^4)] + 5[16128\eta_3 m_b^{10}\omega_3 - 2520\eta_3 m_b^8(15q^2+13s)\omega_3 + 8q^2[(3+90\eta_3+10\eta_4)(q^2-s)^2(q^4 + 5q^2s+2s^2) - 9\eta_3(q^8+17q^6s+42q^4s^2+22q^2s^3+2s^4)\omega_3] + 3m_b^2(20q^4s^2[3-16\eta_4+144(\eta_3+2\eta_3\omega_3)] + q^6s[69+320\eta_4+240\eta_3(6+19\omega_3)-420\eta_4\omega_4] + 3q^2s^3[-9+240\eta_3(-2+3\omega_3)-140\eta_4\omega_4] + 5q^8[-15-16\eta_4+144\eta_3(-3+\omega_3)+84\eta_4\omega_4] + s^4[-27+80\eta_4+240\eta_3(-3+\omega_3)+420\eta_4\omega_4]) + 5m_b^6(s^2[-33+352\eta_4+144\eta_3(-8+33\omega_3)+756\eta_4\omega_4] + q^4[-33+352\eta_4+144\eta_3(-8+47\omega_3) + 756\eta_4\omega_4] + 2q^2s[33+576\eta_3(2+11\omega_3)-4\eta_4(88+189\omega_4)]) + 3m_b^4(-15q^2s^2[1+48(\eta_3+16\eta_3\omega_3) - 12\eta_4(4+7\omega_4)] - 3q^4s[53+1680(\eta_3+3\eta_3\omega_3)-20\eta_4(4+21\omega_4)] + q^6[111+240\eta_3(15-19\omega_3) - 20\eta_4(20+63\omega_4)] + s^3[240\eta_3(9-10\omega_3)-7[-9+20\eta_4(4+9\omega_4)]]])] + 1080m_b^2(m_b^2-q^2)(m_b^2-s)(2m_b^2 - q^2-s)(q^2-s)(6a_2-35\eta_4\omega_4)\Big[-\log\Big(\frac{m_b^2-s}{q^2-s}\Big)+\log\Big(\frac{m_b^2-q^2}{s-q^2}\Big)\Big]\Big]$$

$$\rho^{3p}_{\mathrm{T4}} = \frac{-f_\pi m_b \mu_\pi^2}{24(q^2-s)^6}(m_b^2-q^2)[80\eta_4(q^2-s)[-8m_b^4+q^4-3q^2s-6s^2+m_b^2(q^2+15s)] + 27a_2[45m_b^6+q^6-4q^4s - 30q^2s^2-12s^3-5m_b^4(7q^2+20s)+m_b^2(q^4+68q^2s+66s^2)]]$$

$$\mathrm{T4}_c = \frac{-f_\pi m_b^2 m_b \mu_\pi^2}{160(m_b^2-q^2)^2}e^{-m_b^2/M^2}(12a_2+5[-25+48\eta_3(-10+\omega_3)])$$

---

[1] V. M. Belyaev, A. Khodjamirian, and R. Rückl, Z. Phys. C **60**, 349 (1993); A. Khodjamirian *et al.*, Phys. Lett. B **410**, 275 (1997); E. Bagan, P. Ball, and V. M. Braun, Phys. Lett. B **417**, 154 (1998); A. Khodjamirian *et al.*, Phys. Rev. D **62**, 114002 (2000).
[2] P. Ball and V. M. Braun, Phys. Rev. D **58**, 094016 (1998).
[3] P. Ball, J. High Energy Phys. 09 (1998) 005.
[4] P. Ball and R. Zwicky, J. High Energy Phys. 10 (2001) 019.
[5] V. M. Belyaev *et al.*, Phys. Rev. D **51**, 6177 (1995); A. Khodjamirian *et al.*, Phys. Lett. B **457**, 245 (1999).
[6] P. Colangelo and A. Khodjamirian, hep-ph/0010175; A. Khodjamirian, hep-ph/0108205.
[7] *Proceedings of the 2nd Workshop on the CKM Unitarity Triangle, Durham, England, 2003*, edited by P. Ball *et al.*, eConf C0304052 (2003).
[8] T. Onogi, hep-ph/0309225.
[9] H. Li, hep-ph/0103305; M. Beneke *et al.*, Phys. Rev. Lett. **83**, 1914 (1999); Nucl. Phys. **B606**, 245 (2001).
[10] C. H. Davies, talk at UK BaBar meeting, Durham April 2004 (unpublished).
[11] J. Shigemitsu *et al.*, Nucl. Phys. (Proc. Suppl.) **331**, 129 (2004).
[12] V. L. Chernyak and A. R. Zhitnitsky, Pis'ma Zh. Eksp. Teor. Fiz. **25**, 544 (1977) [JETP Lett. **25**, 510 (1977)]; Yad. Fiz. **31**, 1053 (1980) [Sov. J. Nucl. Phys. **31**, 544 (1980)]; A. V. Efremov and A. V. Radyushkin, Phys. Lett. **94B**, 245 (1980); Teoreticheskaya i Matematicheskaya Fizika **42**, 147 (1980) [Theor. Math. Phys. (Engl. Transl.) **42**, 97 (1980)]; G. P. Lepage and S. J. Brodsky, Phys. Lett. **87B**, 359 (1979); Phys. Rev. D **22**, 2157 (1980); V. L. Chernyak, A. R. Zhitnitsky, and V. G. Serbo, Pis'ma Zh. Eksp. Teor. Fiz. **26**, 760 (1977) [JETP Lett. **26**, 594 (1977)]; Yad. Fiz. **31**, 1069 (1980) [Sov. J. Nucl. Phys. **31**, 552 (1980)].
[13] C.W. Bauer *et al.*, Phys. Rev. D **63**, 114020 (2001).
[14] C.W. Bauer, D. Pirjol, and I.W. Stewart, Phys. Rev. D **67**, 071502 (2003).
[15] M. A. Shifman, A. I. Vainshtein, and V. I. Zakharov, Nucl. Phys. B **147**, 385 (1979); **147**, 448 (1979).
[16] V. M. Braun and I. E. Filyanov, Z. Phys. C **48**, 239 (1990) [Sov. J. Nucl. Phys. **52**, 126 (1990)]; P. Ball, J. High Energy Phys. 01 (1999) 010.
[17] A. Szczepaniak, E. M. Henley, and S. J. Brodsky, Phys. Lett. B **243**, 287 (1990).
[18] E. Braaten, Phys. Rev. D **28**, 524 (1983).
[19] A.S. Kronfeld, Nucl. Phys. (Proc. Suppl.) **129**, 46 (2004).
[20] T. M. Aliev and V. L. Eletsky, Yad. Fiz. **38**, 1537 (1983) [Sov. J. Nucl. Phys. **38**, 936 (1983)]; E. Bagan *et al.*, Phys. Lett. B **278**, 457 (1992).
[21] A. A. Penin and M. Steinhauser, Phys. Rev. D **65**, 054006 (2002); M. Jamin and B. O. Lange, Phys. Rev. D **65**, 056005 (2002).
[22] V. L. Chernyak and A. R. Zhitnitsky, Phys. Rep. **112**, 173 (1984).
[23] V. M. Braun and I. E. Filyanov, Z. Phys. C **44**, 157 (1989) [Sov. J. Nucl. Phys. **50**, 511 (1989)].

[24] S. V. Mikhailov and A. V. Radyushkin, Phys. Rev. D **45**, 1754 (1992).
[25] A. P. Bakulev *et al.*, hep-ph/0405062 [Phys. Rev. D (to be published)].
[26] G. Martinelli and C. T. Sachrajda, Phys. Lett. B **190**, 151 (1987); T. A. DeGrand and R. D. Loft, Phys. Rev. D **38**, 954 (1988); D. Daniel, R. Gupta, and D. G. Richards, Phys. Rev. D **43**, 3715 (1991).
[27] UKQCD Collaboration, L. Del Debbio *et al.*, Nucl. Phys. (Proc. Suppl.) **83**, 235 (2000); L. Del Debbio, M. Di Pierro, and A. Dougall, Nucl. Phys. (Proc. Suppl.) **119**, 416 (2003).
[28] J. Bijnens and A. Khodjamirian, Eur. Phys. J. C **26**, 67 (2002).
[29] A. Khodjamirian, Eur. Phys. J. C **6**, 477 (1999).
[30] A. Schmedding and O. Yakovlev, Phys. Rev. D **62**, 116002 (2000).
[31] A. P. Bakulev, S. V. Mikhailov, and N. G. Stefanis, Phys. Rev. D **67**, 074012 (2003); Phys. Lett. B **578**, 91 (2004).
[32] V. M. Braun, A. Khodjamirian, and M. Maul, Phys. Rev. D **61**, 073004 (2000).
[33] P. Ball and M. Boglione, Phys. Rev. D **68**, 094006 (2003).
[34] J. Charles *et al.*, Phys. Rev. D **60**, 014001 (1999).
[35] D. Becirevic and A. B. Kaidalov, Phys. Lett. B **478**, 417 (2000).
[36] W. A. Bardeen, E. J. Eichten, and C. T. Hill, Phys. Rev. D **68**, 054024 (2003).
[37] A. Abada *et al.*, J. High Energy Phys. 02 (2004) 016.
[38] A. Khodjamirian, in *QCD@Work: International Workshop on Quantum Chromodynamics: Theory and Experiment*, edited by P. Colangelo and G. Nardulli, AIP Conf. Proc. No. 602 (AIP, New York, 2001), p. 194.
[39] D. Becirevic *et al.*, J. High Energy Phys. 01 (2003) 009.
[40] M. B. Voloshin, Yad. Fiz. **50**, 166 (1989) [Sov. J. Nucl. Phys. **50**, 105 (1989)].
[41] D. Becirevic, hep-ph/0211340.
[42] P. Ball, hep-ph/0308249.